การสังเคราะห์ตัวเร่งปฏิกิริยาแพลทินัม-โคบอลต์บนตัวรองรับไทเทเนียด้วยวิธีเฟลมสเปรย์ไพโรไลซิส
สำหรับปฏิกิริยาไฮโดรจิเนชันแบบเลือกเกิดของเฟอร์ฟูรัลเป็นเฟอร์ฟูริลแอลกอฮอล์

นางสาวกิติมา เครือเช้า

วิทยานิพนธ์นี้เป็นส่วนหนึ่งของการศึกษาตามหลักสูตรปริญญาวิศวกรรมศาสตรมหาบัณฑิต
สาขาวิชาวิศวกรรมเคมี ภาควิชาวิศวกรรมเคมี
คณะวิศวกรรมศาสตร์ จุฬาลงกรณ์มหาวิทยาลัย
ปีการศึกษา 2560

SYNTHESIS OF $PtCo/TiO_2$ CATALYSTS BY FLAME SPRAY PYROLYSIS FOR SELECTIIVE HYDROGENATION OF FURFURAL TO FURFURYL ALCOHOL

Miss Kitima Kruachao

A Thesis Submitted in Partial Fulfillment of the Requirements
for the Degree of Master of Engineering Program in Chemical Engineering
Department of Chemical Engineering
Faculty of Engineering
Chulalongkorn University
Academic Year 2017

Thesis Title	SYNTHESIS OF $PtCo/TiO_2$ CATALYSTS BY FLAME SPRAY PYROLYSIS FOR SELECTIIVE HYDROGENATION OF FURFURAL TO FURFURYL ALCOHOL
By	Miss Kitima Kruachao
Field of Study	Chemical Engineering
Thesis Advisor	Professor Joongjai Panpranot, Ph.D.

Accepted by the Faculty of Engineering, Chulalongkorn University in Partial Fulfillment of the Requirements for the Master's Degree

.....Dean of the Faculty of Engineering

(Associate Professor Supot Teachavorasinskun, Ph.D.)

THESIS COMMITTEE

.....Chairman

(Professor Bunjerd Jongsomjit, Ph.D.)

.....Thesis Advisor

(Professor Joongjai Panpranot, Ph.D.)

.....Examiner

(Associate Professor Anongnat Somwangthanaroj, Ph.D.)

.....External Examiner

(Assistant Professor Okorn Mekasuwandumrong, D.Eng.)

กิติมา เครือเข้า : การสังเคราะห์ตัวเร่งปฏิกิริยาแพลทินัม-โคบอลต์บนตัวรองรับไทเทเนียด้วยวิธีเฟลมสเปรย์ไพโรไลซิสสำหรับปฏิกิริยาไฮโดรจิเนชันแบบเลือกเกิดของเฟอร์ฟูรัลเป็นเฟอร์ฟูริลแอลกอฮอล์ (SYNTHESIS OF $PtCo/TiO_2$ CATALYSTS BY FLAME SPRAY PYROLYSIS FOR SELECTIIVE HYDROGENATION OF FURFURAL TO FURFURYL ALCOHOL) อ.ที่ปรึกษาวิทยานิพนธ์หลัก: ศ. ดร. จูงใจ ปั้นประณต, 84 หน้า.

ปฏิกิริยาไฮโดรจิเนชันแบบเลือกเกิดของเฟอร์ฟูรัลเป็นเฟอร์ฟูริลแอลกอฮอล์ดำเนินการที่อุณหภูมิ 50 องศาเซลเซียส ความดัน 20 บาร์ โดยใช้ตัวเร่งปฏิกิริยาแพลทินัมโคบอลต์บนตัวรองรับไทเทเนียที่มี 0.5 เปอร์เซ็นต์โดยน้ำหนักของแพลทินัม และ0-0.8เปอร์เซ็นต์โดยน้ำหนักของโคบอลต์ วิเคราะห์คุณลักษณะของตัวเร่งปฏิกิริยาด้วยเทคนิคการเลี้ยวเบนของรังสีเอ็กซ์ การดูดซับทางกายภาพด้วยแก๊สไนโตรเจน เอ็กซเรย์โฟโตอิเล็กตรอนสเปกโตรสโกปี การรีดักชันของไฮโดรเจนด้วยการโปรแกรมอุณหภูมิ อะตอมมิกแอบซอร์พชันสเปกโตสโกปี การดูดซับทางเคมีด้วยแก๊สคาร์บอนมอนอกไซด์ และ กล้องจุลทรรศน์อิเล็กตรอนแบบส่องผ่าน การเติมโคบอลต์ลงในตัวเร่งปฏิกิริยาแพลทินัมบนตัวรองรับไทเทเนียด้วยวิธีเคลือบฝังจะเพิ่มทั้งค่าการเปลี่ยนของเฟอร์ฟูรัลและค่าการเลือกเกิดของเฟอร์ฟูริลแอลกอฮอล์เพราะจะไปป้องกันการเปลี่ยนโครงสร้างผลึกจากอะนาเทสเป็นรูไทล์ของไทเทเนียและเพิ่มอันตรกิริยาระหว่างโลหะกับไทเทเนีย ส่วนการเติมโคบอลต์ลงในตัวเร่งปฏิกิริยาแพลทินัมบนตัวรองรับไทเทเนียด้วยวิธีเฟลมสเปรย์ไพโรไลซิส ทำให้ค่าการเปลี่ยนของเฟอร์ฟูรัลลดลงแต่เพิ่มค่าการเลือกเกิดของเฟอร์ฟูริลแอลกอฮอล์เพราะระหว่างการเฟลมสเปรย์ไพโรไลซิสการเติมโคบอลต์จะไปเร่งการเปลี่ยนโครงสร้างผลึกจากอะนาเทสเป็นรูไทล์ เปรียบเทียบผลของวิธีเตรียมพบว่าตัวเร่งปฏิกิริยาแพลทินัมบนตัวรองรับไทเทเนียสังเคราะห์ด้วยวิธีเฟลมสเปรย์ไพโรไลซิสและวิธีเคลือบฝังแสดงค่าการเปลี่ยนของเฟอร์ฟูรัลใกล้เคียงกันแต่ค่าการเลือกเกิดของเฟอร์ฟูริลแอลกอฮอล์ของตัวเร่งปฏิกิริยาแพลทินัมบนตัวรองรับไทเทเนียด้วยวิธีเฟลมสเปรย์ไพโรไลซิสสูงกว่าวิธีเคลือบฝังเนื่องจากตัวเร่งปฏิกิริยาแพลทินัมบนตัวรองรับไทเทเนียด้วยวิธีเฟลมสเปรย์ไพโรไลซิสมีอันตรกิริยาระหว่างแพลทินัมกับไทเทเนียที่แข็งแรงกว่า ตัวเร่งปฏิกิริยาแพลทินัม-0.2โคบอลต์ที่สังเคราะห์ด้วยวิธีเคลือบฝังแสดงประสิทธิภาพทางตัวเร่งปฏิกิริยาดีที่สุด สรุปผล ความว่องไวในการไฮโดรจิเนชันจะเพิ่มขึ้นเมื่อเพิ่มเปอร์เซ็นต์อะนาเทสของตัวรองรับไทเทเนียในขณะที่ค่าการเลือกเกิดของเฟอร์ฟูริลแอลกอฮอล์ส่วนใหญ่ขึ้นอยู่กับอันตรกิริยาระหว่างโลหะกับไทเทเนียที่แข็งแรง

ภาควิชา วิศวกรรมเคมี ลายมือชื่อนิสิต .....

สาขาวิชา วิศวกรรมเคมี ลายมือชื่อ อ.ที่ปรึกษาหลัก .....

ปีการศึกษา 2560

5970111721 : MAJOR CHEMICAL ENGINEERING

KEYWORDS: PT/TIO2 / PT-CO/TIO2 / LIQUID-PHASE SELECTIVE HYDROGENATION / FURFURAL / FLAME SPRAY PYROLYSIS

KITIMA KRUACHAO: SYNTHESIS OF $PtCo/TiO_2$ CATALYSTS BY FLAME SPRAY PYROLYSIS FOR SELECTIIVE HYDROGENATION OF FURFURAL TO FURFURYL ALCOHOL. ADVISOR: PROF. JOONGJAI PANPRANOT, Ph.D., 84 pp.

The selective hydrogenation of furfural to furfuryl alcohol (FA) was carried out in a batch reactor at 50 °C and 20 bar H_2 using Pt-Co/TiO_2 with 0.5 wt%Pt and 0-0.8 wt%Co. The catalysts were characterized by X-ray diffraction (XRD), N_2-physisorption, X-ray photoelectron spectroscopy (XPS), H_2-temperature programmed reduction (H_2-TPR), atomic absorption spectroscopy (AAS), CO-pulse chemisorption and transmission electron microscopy (TEM). Addition of Co into monometallic (I) Pt/TiO_2 catalyst increased both furfural conversion and FA selectivity because it prevented anatase to rutile transformation of TiO_2 and increased the interaction between metal and TiO_2. However, Co adding into monometallic (F) Pt/TiO_2 catalyst resulted in a decrease in furfural conversion but increased FA selectivity because during FSP, Co addition accelerated anatase to rutile transformation. A comparison between flame spray pyrolysis and impregnation method showed that, the (F) Pt/TiO_2 and (I) Pt/TiO_2 catalysts exhibited similar furfural conversion but FA selectivity of the (F) Pt/TiO_2 was much higher than the (I) Pt/TiO_2 because the (F) Pt/TiO_2 catalyst showed stronger interaction between Pt and TiO_2 support. For bimetallic catalysts, the Pt-0.2Co/TiO_2 catalysts synthesized by impregnation method exhibited the best catalytic performance for selective hydrogenation of furfural to furfuryl alcohol. In summary, hydrogenation activity increased with increasing %anatase in the TiO_2 support while FA selectivity depended largely on the strong metal-support interaction.

Department:	Chemical Engineering	Student's Signature	.....
Field of Study:	Chemical Engineering	Advisor's Signature	.....
Academic Year:	2017		

ACKNOWLEDGEMENTS

I really appreciate to my thesis advisor, Professor Joongjai Panpranot, for her valuable suggestions, assistance, encouragement and made my thesis completed. In addition, I would also be grateful to Professor Bunjerd Jongsomjit as the chairman, Associate Professor Anongnat Somwangthanaroj and Assistant Professor Okorn Mekasuwandumrong as the member of Thesis committee and for your brilliant comments and suggestions.

Moreover, I would like to acknowledge to my parent and my friends both from Chulalongkorn University and from Silpakorn University for all their support throughout the period of this research.

Finally, I gratefully thank the financial supports from the Thailand Research Fund (TRF), the Ratchadaphiseksomphot Endowment Fund for International Research Integration and Chulalongkorn University.

CONTENTS

Page

Page

Page

Page

LIST OF TABLES

Page

LIST OF FIGURES

Page

CHARPTER I

INTRODUCTION

1.1 Introduction

Renewable biomass is interesting to use as feedstock instead of fossil fuels because nowadays fossil fuels are mainly used as precursors in the production of many petrochemical products but they are unsustainable and caused global warming. Biomass can be converted to many chemicals such as cellulose, vanillin, and furfural. Furfural can be produced on large industrial scales by taking plant mass and treating it with an acid. Furfural is an aldehyde of furan and is a yellow oily liquid in pure form, but tends to turn brown upon prolonged exposure to air and moisture. An aldehyde is an organic functional group that has a carbonyl group (carbon-oxygen double bond) attached to a hydrogen and some other carbon-based side chains. Furfural is a biomass-derived chemicals, received by acid-catalyzed dehydration of xylose, the main building-block of hemicellulose constituent of lignocellulose [1].

The selective hydrogenation of furfural to furfuryl alcohol (FA) is the reaction of interest. The compound consists of two functional group a C=C double bond and C=O double bond. To produce FA, furfural is hydrogenated at C=O bond and transformed to FA. The selective hydrogenation of furfural to FA is an interesting reaction for producing lysine, furan resins, lubricant oils, and ascorbic acid. In the present industrial process, copper chromate was used as a catalyst for furfural hydrogenation to furfuryl alcohol under operating conditions between 130 and 200 °C at pressures up to 30 bar. Although copper chromate shows high conversion and selectivity to FA but Cr_2O_3 is toxic and affects the waste disposal. Alternatively, the catalytic processes should operate at mild conditions using less toxic catalyst. Precious metal catalysts have been investigated for the gas phase and liquid phase hydrogenation of furfural, including Pd, Ru, Co and Pt because they showed high catalytic activity and selectivity to the desire product and can be operated at mild conditions. Platinum (Pt) catalysts are commonly used in the selective hydrogenation

of furfural because of their high catalytic activity, however, they usually give medium selectivity of FA [2].

Bimetallic catalyst is interesting in selective hydrogenation reaction because adding of second metal into monometallic catalyst will promote positive effect in term of conversion and selectivity. For Pt based catalysts, popular second metals for hydrogenation included Pt-Sn[3], Ni-Pt[4], Pt-Re[5] and Pt-Co[6, 7]. Cobalt (Co) is an interesting promoter for platinum catalysts. For example, Zheng, R. et al.[6] reported that Pt-Co showed higher hydrogenation activity and selectivity towards C=O bond hydrogenation than the corresponding monometallic Pt catalysts in cinnamaldehyde hydrogenation reaction. The addition of Co to Pt may be useful for improving the hydrogenation of C=O to produce FA in the selective hydrogenation of furfural.

Flame spray pyrolysis technique (FSP) is known as a one-step method for the synthesis of nanoparticles. The advantages of FSP are that the nanoparticles made from FSP have high purity, relatively narrow size distribution, strong metal interaction and their properties can be tailored by controlling the synthesis conditions such as precursor concentration and dispersion gas flow rate[8, 9]. Somboonthanakij, S. et al. [10] reported that Pd/SiO_2 from FSP method showed higher catalytic performances than impregnation catalyst in liquid-phase hydrogenation of 1-heptyne. Pisduangdaw, S. et al [11] also reported that flame made Pt-Sn/Al_2O_3 showed higher catalytic performances than impregnation catalyst in the liquid-phase hydrogenation of dehydrogenation of propane. It can be seen that the FSP-made catalysts have shown high catalytic performances in hydrogenation reactions than the catalysts prepared by the conventional impregnation method.

In this work, Pt/TiO_2 and PtCo/TiO_2 were prepared by FSP and impregnation methods and tested in the selective hydrogenation of furfural to FA. The effects of Co adding into Pt based catalyst and the different preparation methods of catalysts on the catalytic properties were investigated by several characterization such as techniques N_2 physisorption, X-ray diffraction (XRD), CO pulse chemisorption and H_2-temperature-programmed reduction (H_2-TPR).

1.2 Objectives of the Research

To study the characteristics and catalytic properties of Pt/TiO_2 and $Pt\text{-}Co/TiO_2$ catalysts synthesized by one-step flame spray pyrolysis in comparision to impregnation method in the selective hydrogenation of furfural to furfuryl alcohol.

1.3 Scopes of the Research

1.3.1 Preparation of Pt/TiO_2 catalysts by flame spray pyrolysis and impregnation with Pt content 0.5 wt% and evaluation of the catalytic performance of the flame- and impregnation-made catalysts after reduction at 500 $^{\circ}C$ in the hydrogenation of furfural in a batch reactor at constant temperature and pressure 50$^{\circ}C$ and 20 bar in hydrogen.

1.3.2 Preparation of $Pt\text{-}Co/TiO_2$ catalysts by flame spray pyrolysis and co-impregnation with Pt content 0.5 wt% and Co loading 0-0.2 wt% and evaluation of the catalytic performance of the flame- and impregnation-made catalysts after reduction at 500 $^{\circ}C$ in the hydrogenation of furfural in a batch reactor at constant temperature and pressure 50$^{\circ}C$ and 20 bar in hydrogen.

1.3.3 Characterization of the prepared catalysts by various methods including

1.3.3.1 N_2 physisorption

1.3.3.2 X-ray diffraction (XRD)

1.3.3.3 CO pulse chemisorption

1.3.3.4 Atomic absorption spectroscopy (AAS)

1.3.3.5 H_2-temperature programmed reduction (H_2-TPR)

1.3.3.6 Transmission electron spectroscopy (TEM)

1.3.3.7 X-ray photoelectron spectroscopy (XPS).

1.4 Research Methodology

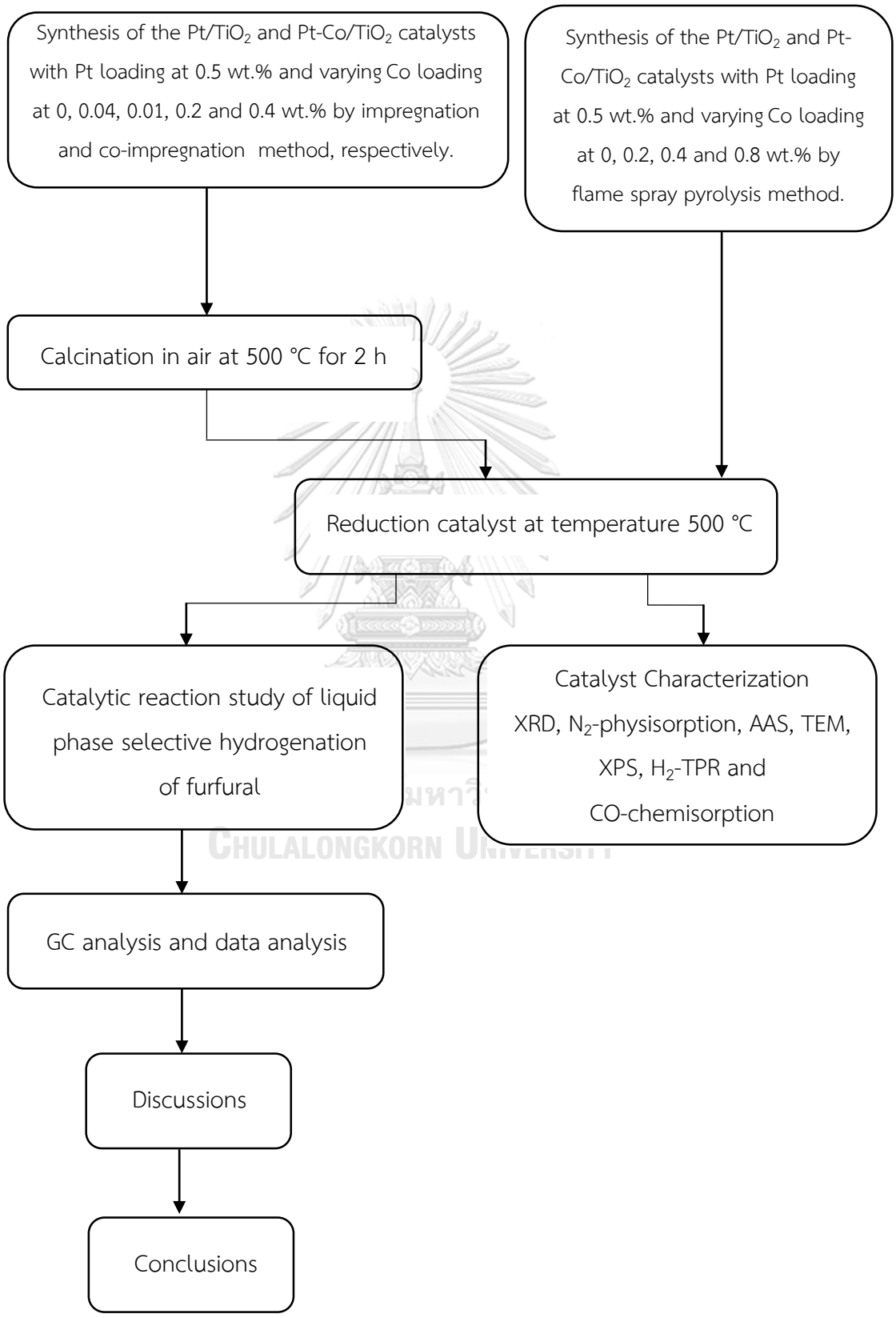

CHARPTER II

BACKGROUND AND LITERITURE REVIEW

2.1 Hydrogenation with heterogeneous catalysts

Hydrogenation is chemical reaction between hydrogen molecule and unsaturated organic compound. This process is useful in pharmaceutical and petrochemical industry. Catalysts used in this reaction can be either heterogeneous or homogeneous. Heterogeneous catalysts for hydrogenation are more commonly used in industry because reactant and catalyst are in different phases providing easily separation from product. In homogeneous catalysts, catalyst is dissolved in reactant or the catalyst is in the same phase as the reactants.

Generally, the adsorption of chemicals onto the catalyst surface takes place in two stages: physisorption characterized by weak forces (van der Waals) and chemisorption that involves the formation of chemical bonds. Metals commonly used in heterogeneous catalytic hydrogenation are palladium, platinum, rhodium, nickel, cobalt, and ruthenium. Addition of a second metal into the main catalyst affects the catalyst activity and selectivity. Heterogeneous catalysts may be unsupported or supported. For supported catalysts, the metal is deposited on an inert material such as carbon, graphite, alumina or inorganic salts. Examples of platinum support are carbon-carbon and carbon-heteroatom double bonds for the reduction of aromatic systems [12].

The advantages of heterogeneous catalyst are their relatively low price, easy separation, and high thermal stability compared to homogeneous catalyst [13]. Heterogeneous catalyst can be separated by simple separation such as filtration or used fix bed reactor in gas phase reaction. In contrast, the separation for homogeneous catalyst is difficult and complex system such as liquid-liquid extraction, ion-exchange, and distillation is necessary.

2.2 Properties of platinum

Platinum is a chemical element with symbol Pt and atomic number 78. It is a lustrous silvery-white, malleable, ductile metal and a member of group 10 of the periodic table of the elements and it has six naturally occurring isotopes. Platinum is one of the least reactive metals and has remarkable resistance to corrosion, even at high temperatures, therefore, it is considered a noble metal. Platinum metal has a number of useful properties, which explains its application in a wide range of industries such as catalytic converters, laboratory equipment, electrical contacts and electrodes, platinum resistance thermometers, dentistry equipment, and jewelry.

Platinum supported catalysts are widely used in hydrogenation reaction. Platinum catalyst has 2 forms: supported and unsupported catalyst. Supported catalyst is recommended to obtain maximum efficiency of the metal. In general, platinum supported catalysts show higher activity and greater resistance to poisoning than platinum unsupported catalyst [14].

Table 2.1 Physical Properties of Platinum [15]

Physical Properties	
Atomic number	78
Atomic weight	195
Electron configuration	$[Xe]4f^{14}5d^{9}6s^{1}$
Electronegativity	2.28
Crystal structure	Face centered cubic (fcc)

Melting point	1768 ℃
Boiling point	3825 ℃

2.3 Study on TiO_2 as a catalyst support

Titanium dioxide (TiO_2) is widely used as catalyst support and used in many reactions such as hydrogenation, dehydrogenation and photocatalyst under UV light in the degradation of organic pollutants. It is very interesting support for hydrogenation reaction because it shows the strong metal support interaction (SMSI) effect at high reduction temperature [16]. TiO_2 synthesis techniques usually require high temperatures to crystallize the amorphous material into one of the phases of TiO_2, such as brookite, anatase, and rutile, consequently leading to larger particles and typically nonporous materials. The advantages of titanium dioxide are nontoxicity, long-termphoto stability, and high effectiveness so it has been widely utilized in mineralizing toxic and nonbiodegradable environmental contaminants [17]. In commercial support, P25 is interesting support because it shows high activity for many kinds of photocatalytic reactions and has been used in many studies. P25 consists of anatase and rutile phases [18].

Ananthan, S.A. et al.(2011) [19] studied the Ru/TiO_2 and Pt/TiO_2 nanocatalysts prepared by impregnation method and reduced at two different temperatures, 375°C and 575°C. Activity and selectivity of the catalysts were evaluated in liquid phase selective hydrogenation of citral. The $1.5\%Pt/TiO_2$ reduced at 575°C showed higher selectivity of unsaturated alcohols (hydrogenated C = O) because of the influence of strong metal support interaction (SMSI effect) of the catalysts towards the selective activation of C=O hydrogenation. The reduction temperature caused the occurrence of TiO_x or presence of partially reduced species in TiO_2 which promoted the hydrogenation of C=O bond. The occurrence of unsaturated Ti cation strengthened the interaction of the C=O bond with the catalyst resulting high selectivity of C=O bond.

Claus, P. et al. (1997) [20] studied Pt supported TiO_2 catalyst prepared by ion-exchange or sol-gel technique. Reduction at 200°C or 500°C was found alter to the phase composition of titania (anatase and rutile). The catalytic performances of the prepared catalysts were investigated in gas phase selective hydrogenation of crotonaldehyde at 140 °C and 2 MPa of H_2. It was found that the phase composition of the support has a strong influence on the activity in which the catalytic activity decreased with increasing anatase fraction. The higher reduction temperature (500 °C) showed higher activing than the catalyst reduced at low reduced temperature (200 °C) as the result of SMSI effect which may also alter the selectivity towards the unsaturated alcohol. Such effect was more pronounced by the close contact of Pt with in the anatase matrix.

Englisch, M. et al. (1997)[21] studied SiO_2-and TiO_2-supported Pt catalysts prepared by ion exchange technique. The catalytic performances of catalysts were tested in hydrogenation of crotonaldehyde. The selectivity is concluded to be directly controlled by the adsorption structure of crotonaldehyde. The selectivity to the unsaturated alcohol increases with increasing particle size. The selectivity of Pt/TiO_2 catalysts is then determined by the metal particle size and the extent of decoration of Pt with TiO_x particles (SMSI state). In the case of large particles, the prevalent dense Pt(111) surface planes of Pt constrain the sorption of the C=C double bond which enhances the selectivity to hydrogenate the C=O double bond. The presence of coordinatively unsaturated Ti cations in these oxide particles enhances the sorption strength of the C=O bond, resulting in an enhanced selectivity to crotyl alcohol.

2.4 Flame spray pyrolysis synthesis

Flame spray pyrolysis technique (FSP) is known as a one-step method for the synthesis of nanoparticles. FSP is a gas phase combustion synthesis method enabling the production of a broad range of materials in the form of nanostructured powders with high specific surface area and primary particle size in the range of few nanometers. Powder from FSP process has been applied for the production of powders industrially and can controlled characteristics at a high rate.

Procedures of FSP process is based on the exothermic combustion of a spray of a mixture liquid precursor. By means of a suitable nozzle-equipped burner, a liquid-phase mixture containing a metallorganic compound and a solvent is dispersed into a flame where the resulting mixture droplets are combusted generating small clusters, which grow up by collisions and sintering processes taking place in the high temperature environment of the flame. An additional oxygen flow provides both the complete combustion of the solvent and the metallorganic compound in water and CO_2. Due to the oxygen abundance and the high temperatures of the flame, FSP-made nanoparticles are typically fully oxidized and crystalline. Powders are collected by a suitable filtering system placed above the flame. A schematic of experimental set-up of FSP is shown in Figure 2.1 The apparatus consists of an external-mixing gas nozzle made from a tube of outer diameter 0.91 mm (inner diameter 0.6 mm). It is settled in an opening of 1.2 mm in diameter making an annular gab of 48 mm^2 maximum area. Precursor and fuel flow through the tube while dispersion gas flow though the annular gab. The droplet size can be controlled by adjustment by dispersion gas or liquid flow rate. The products are corrected on a glass fiber filter and then the gas flow though the filter which is maintain by vacuum pump.

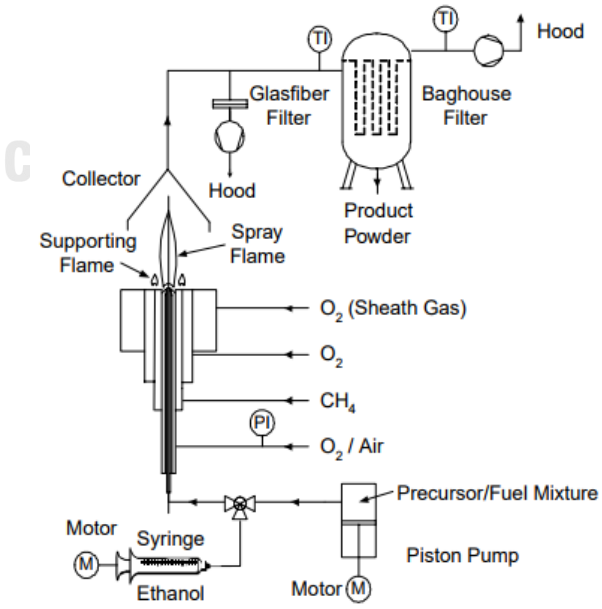

Figure 2.1 Schematic of Flame spray pyrolysis (FSP) [22].

Formation of particle during flame spray pyrolysis is shown in Figure 2.2 The mechanism of flame-made formation is explained as follow: A liquid precursor was injected in the flame though a two-phase nozzle and dispersed to be fine droplets by dispersion gas. Then the fine droplets were evaporated and combusted when the met the flame. Afterward subsequent, nucleation and growing particle by coagulation and condensation were occurred along the axial direction of the flame. The various properties of the FSP product have a large range and can be change by selecting precursor condensation, feed rate and dispersion gas flow rate.

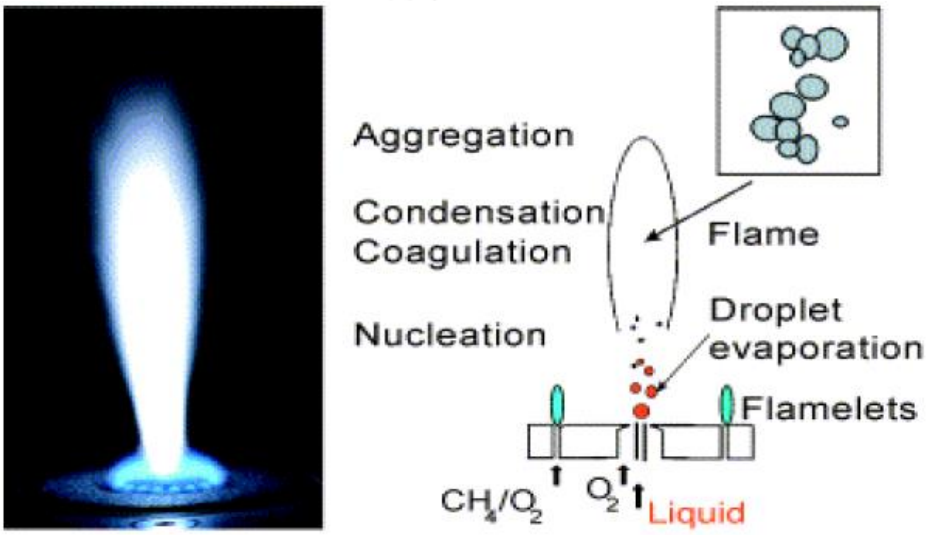

Figure 2.2 Particle formation during flame spray pyrolysis synthesis [22].

The advantages of FSP are that the nanoparticles made from FSP have high purity and relatively narrow size distribution and their properties can be tailored by controlling the synthesis conditions such as precursor concentration and dispersion gas flow rate [8, 9]. And no post-production treatment steps are required and the nanoparticles are ready to use. The FSP-made catalysts have shown high catalytic performances in hydrogenation reactions than the catalysts prepared by the conventional impregnation method [10]. Many researchers have suggested the preparation catalysts by FSP and showed significant physiochemical properties and

their good catalytic performance in different reactions. Nanoparticles from FSP have been applied in various types of catalytic reactions as shows in Table.

For example, Somboonthanakij, S. et al. (2007) [10] studied SiO_2 supported Pd catalysts prepared by one-step flame spray pyrolysis for liquid-phase hydrogenation of 1-heptyne and compared with conventional catalyst from impregnation method. They found that flame made catalysts showed higher catalytic activities for selective hydrogenation of 1-heptyne under mild conditions than the conventional prepared Pd/SiO_2 catalyst. Pd dispersion affected to alkyne hydrogenation activity that when Pd dispersion was increased, the conversion was increased.

Pisduangdaw, S. et al. (2007) [23] studied nanocrystalline Pt/TiO_2 catalysts synthesized by the single-step flame spray pyrolysis (FSP) method for liquid-phase selective hydrogenation of 3-nitrostyrene compared with catalyst from sol-gel and impregnation method. The catalysts were reduced at 200 ℃ or 500 ℃. From the results, Pt/TiO_2 from FSP method had higher dispersion of Pt, small particle size of Pt and higher anatase/rutile ratio. FSP-made catalysts showed improved catalytic performance in terms of both hydrogenation activity and selectivity to vinylaniline (VA) which improved from 61 to 66% and from 40 to 73% by reduction at high temperature (500℃). When compared with sol-gel and impregnation catalyst. They found that both of sol-gel and impregnation catalyst had higher amount of rutile phase composition and much lower Pt dispersion which affected to lower hydrogenation activity than flame made catalysts.

Liu, G. et al. (2013) [24] studied Ce–Mn oxides catalysts from flame spray pyrolysis (FSP) and tested in the catalytic oxidation of benzene and compared to other Ce-Mn oxides with varying cerium/magnesium ratios. They found that flame-made Ce–Mn oxide exhibited high catalytic activity for benzene oxidation comparable to Ce–Mn oxides with different cerium-to-manganese ratios because of strong interaction between cerium and manganese oxides within the catalyst particles which was ascribed to Ce and Mn species well mixing during high temperature FSP process.

Mekasuwandumrong, O. et al. (2013) [25] studied Pd/TiO_2 catalyst synthesized by one-step flame spray pyrolysis and their catalytic performances in the liquid-phase

selective hydrogenation of 1-heptyne compared to the ones prepared by conventional impregnation. They found that Pd/TiO_2 from FSP method showed significant physiochemical properties and good catalytic performance in this reaction. Flame made catalyst showed higher selectivities to 1-heptene at complete conversion of 1-heptyne than impregnation of palladium on the FSP-synthesized and the commercial (P-25) TiO_2 supports because FSP synthesis improved catalytic properties of Pd/TiO_2, which were attributed to a stronger interaction and intimate contact between the very fine Pd particles and the TiO_2 support.

Schimmoeller, B. et al. (2010) [26] studied vanadia/titania (V_2O_5/TiO_2) catalysts with varions vanadia loadings synthesized by flame spray pyrolysis (FSP) and compared with wet impregnation catalyst for oxidation of chlorobenzene. For dispersion, flame-made catalysts showed higher VO_x species than wet-impregnated catalysts. V_2O_5/TiO_2 catalysts from FSP technique with varying vanadia loadings showed no crystallitne V_2O_5 species and high VO_x species dispersion. For catalytic performance, when increasing vanadia loading at constant SSA of both FSP and wet impregnation catalyst, the activity in term of catalytic total combustion of chlorobenzene increased.

Table 2.2 Application of flame spray pyrolysis catalyst in various reactions

Heterogeneous catalyst	Reaction	Reference
$Pd/SiO_2–Al_2O_3$	Hydrogenation of acetophenone	[27]
$Pd–Pt/Al_2O_3$	Methane combustion	[28]
CuO	Photoelectrochemical water splitting	[29]
TiO_2 and Au/TiO_2	Photocatalytic hydrogen production	[30]
$Pt–Sn/Al_2O_3$	Dehydrogenation of propane	[11]

Co/Al_2O_3	Fischer–Tropsch	[31]
Ag/ZnO	UV-photodegradation of methylene blue	[32]
Pt/Al_2O_3	hydrogenation of ethyl pyruvate	[33]
Ni/SiO_2	Carbon Dioxide Reforming of Methane	[34]

2.5 Effect of Co-modified catalyst on catalyst properties and catalytic performance

Cobalt is a chemical element with symbol Co and atomic number 27. It is similar to iron and nickel in its physical properties It is a member of group VIII of the periodic table. Physical properties of Co is a brittle, hard, silver-grey transition metal with magnetic properties similar to those of iron (it is ferromagnetic). It has a high melting point and is hard-wearing even at high temperatures. Its alloys also possess useful properties and so it finds use in high speed steels and cutting tools for instance. Application of cobalt is the production of high performance alloys such as Cobalt-based superalloys, Batteries, Pigments and coloring, catalyst and others [35].

Table 2.3 Physical Properties of Co [36].

Physical Properties	
Atomic number	27
Atomic weight	59
Electron configuration	[Ar] $3d^7$ $4s^2$

Electronegativity	1.88
Crystal structure	hexagonal close-packed
Melting point	1495 ℃
Boiling point	2927 ℃

Zheng, R. et al. (2012) [6] studied Co-Pt/SiO_2 and Cu- Pt/SiO_2 bimetallic and Co, Cu, Pt monometallic catalysts prepared by impregnation method in liquid phase hydrogenation of cinnamaldehyde. Characterization, the results showed that the presence of Pt facilitates the reduction of 3d metals (Co or Cu) from H_2-TPR. The reaction test results showed that Co-Pt and Cu-Pt bimetallic catalysts exhibit much higher hydrogenation activity than the corresponding monometallic catalysts, and Co-Pt shows much higher selectivity towards C=O bond hydrogenation than Cu-Pt. The result from CO chemisorption measurements showed that Co-Pt possesses significantly higher CO chemisorption capacity compared to monometallic catalysts.

Bertero, N. M. et al. (2009) [37] studied carbon supported on Pt–Co bimetallic and monometallic catalysts with varying Pt/(Pt + Co) ratios and a fixed total metal loading of about 2% by impregnation and co-impregnation. The performance catalysts were tested in liquid-phase hydrogenation of citral (393 K and 10 bar). Pt/C and Co/C monometallic catalysts showed very low activity and selectivity to the desired products leading to side reactions, such as citral decarbonylation and hydrogenolysis. The bimetallic Pt–Co/C has proved to be very active and selective to geraniol/nerol and the main products detected were geraniol/nerol, citronellal and citronellol. It is suggested that cobalt improves the catalytic performance of platinum by electron transfer. This electron transfer is favored by the high interaction of both metals existing in these types of bimetallic compounds.

Pisduangdaw, S. et al. (2015) [7] studied bimetallic Pt–Co/TiO_2 and monometallic catalysts with Pt at 0.5 wt.% and Co loadings varying at 0, 0.1, 0.2, and 0.5 wt.% synthesized by flame spray pyrolysis technique compared with impregnation catalysts in the selective hydrogenation of 3-nitrostyrene. In this work, the catalysts were reduced at 200 °C and 500 °C. For bimetallic Pt–Co/TiO_2, they found that when reduced catalyst at 500 °C both conversion of 3-nitrostyrene and selectivity of vinylaniline over Pt–Co/TiO_2 were drastically increased and surpassed those of monometallic Pt/TiO_2 due to the strong interaction between Pt–Co and the migration of TiO_x species.

Borgna, A. et al. (2004) [38] studied silica-supported Pt-Co bimetallic catalysts with various Pt/Co ratios prepared using the spin-coating technique for liquid phase selective hydrogenation of crotonaldehyde. Addition of cobalt in monometallic catalysts resulted in an increased selectivity of unsaturated alcohol (crotyl alcohol) because cobalt promoted the C=O hydrogenation. Selective hydrogenation of crotonaldehyde requires the use of promoted Pt catalysts since promoters are indispensable to activate the C=O group. They found that the activation mechanism of the C=O group in Pt-Co model catalysts involves the formation of Pt-Co alloyed clusters.

2.6 Hydrogenation of furfural over heterogeneous catalyst

The selective hydrogenation of furfural to furfuryl alcohol is an important reaction for industrial producing lysine, furan resins, lubricant oils, and ascorbic acid. In this reaction, the desired selective hydrogenation product furfuryl alcohol was observed as well as the side reaction products which occurred from the methanol reaction forming solvent product (SP) as shown in Figure.4. Furfural is hydrogenated at C=O bond transformed to furfuryl alcohol after that furfuryl alcohol is hydrogenated at both C=C bond transformed to tetrahydrofurfuryl alcohol However, when using methanol as a solvent, 2-furaldehyde dimethyl acetal (solvent product) may be formed.

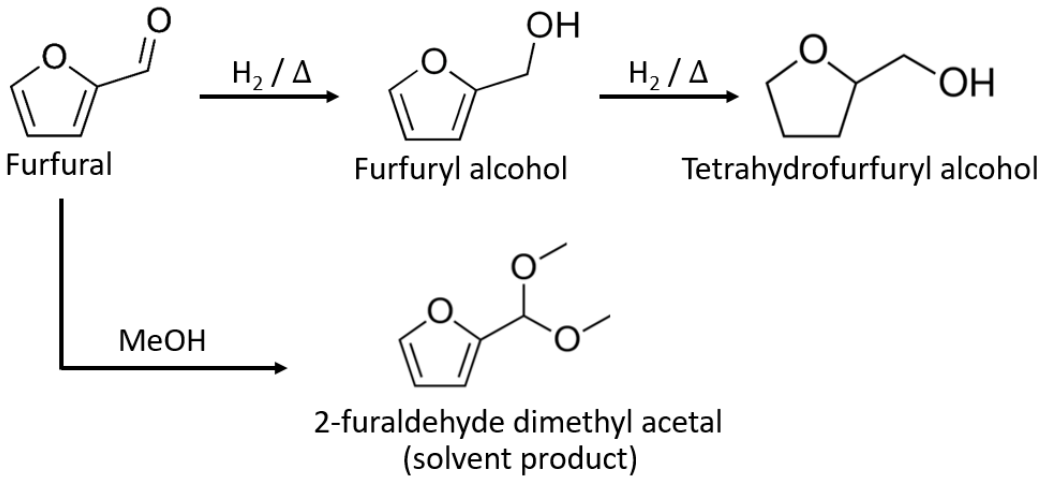

Figure 2.3 Simplified reaction scheme of the hydrogenation of furfural.

Resin Lubricant oil Vitamin C

Figure 2.4 Applications of furfuryl alcohol

Table 2.4 Summary of the research of selective hydrogenation of furfural on various catalysts under different reaction conditions.

Researchers	Studies	Catalyst and preparation method	Reaction condition	Results
Taylor, M. J. et al. (2016) [2]	Studied Pt nanoparticles supported on SiO_2, ZnO, ɣ-	Pt/SiO_2, Pt/ZnO, $Pt/ɣ\text{-}Al_2O_3$, Pt/CeO_2 were	T=50 °C P_{H2}= 1 atm	$Pt/ɣ\text{-}Al_2O_3$ catalyst showed best performance in methanol as a

	Al_2O_3, CeO_2 for selective liquid phase hydrogenation of furfural to furfuryl alcohol under extremely mild conditions	prepared by adapting the method of Jones, et al	Reaction time = 7 h	solvent with conversion of furfural = 80% and selectivity of furfuryl alcohol = 99%.
Merlo, A. B. et al. (2009) [3]	Studied the effect of Sn adding on Pt/SiO_2 (varying Sn/Pt ratio) for liquid-phase hydrogenation of furfural	Pt/SiO_2, $PtSn/SiO_2$ were prepared by ion-exchange and then added Sn by controlled surface reactions technique	T=100 °C P_{H2}=10atm Reaction time = 8 h	The best performance was achieved in $PtSn/SiO_2$ at Sn/Pt ratio = 0.3 with reaction rate = 2.3 mmol gPt^{-1} s^{-1} and selectivity of furfuryl alcohol = 98.7%. (reaction rate estimated between 0% and 10% conversion)
Zhang, C. et al. (2017) [4]	Studied the effect of preparation of bimetallic catalyst (Ni-	- $Cu@Pt/SiO_2$ and $Ni@Pt/SiO_2$ were prepared by	T=250 °C P_{H2}=6.9 atm	$Cu@Pt/SiO_2$ and $Ni@Pt/SiO_2$ overlayer catalysts showed higher reactivity in

	Pt/SiO_2 and Cu-Pt/SiO_2) preparation of monometallic catalysts (Ni/SiO_2, Cu/SiO_2 and Pt/SiO_2) and condition for selective hydrogenation of furfural to furfuryl alcohol	directed deposition technique - Ni/SiO_2, Cu/SiO_2 and Pt/SiO_2 were prepared by impregnation	Reaction time = 1.5 h	furfural conversion and furfuryl alcohol selectivity compared to their parent
Bhogeswararao, S. et al. (2015) [1]	Studied the effect of temperatures of reaction of ɣ-Al_2O_3-supported Pt and Pd catalysts and varied concentration of metal loading in hydrogenation of furfural	Pt/ɣ-Al_2O_3 and Pd/ɣ-Al_2O_3 were prepared by wet impregnation method	T=25°C and ≥180 °C P_{H2}=20atm Reaction time = 8 h	- At temperature reaction = 25 °C, Pt/ɣ-Al_2O_3 catalysts were selective for hydrogenation of C=O group, Pd/ɣ-Al_2O_3 catalysts hydrogenated both ring and C=O bonds of furfural - At temperature reaction ≥180 °C, the supported Pd catalysts enabled decarbonylation

				of FAL giving furan in 82% yield.
Musci, J. J. et al. (2017) [39]	Studied the effect of Sn adding in carbon-supported monometallic Ru and varied Sn/Ru ratio for aqueous phase hydrogenation of furfural	Ru/C and RuSn/C were prepared by impregnation method	T=90 °C P_{H2}=12.5 atm Reaction time = 6 h	RuSn0.4/C (Sn/Ru ratio = 0.4) catalyst showed highest performance both of furfural conversion (91 %)and furfuryl alcohol selectivity(90%)
Fulajtárova, K. et al. (2015) [40]	Studied the monometallic (Pd, Cu) and bimetallic Pd–Cu catalysts with different metals loadings on various supports and various preparation method of support for the selective hydrogenation of furfural to furfuryl alcohol	monometallic (Pd, Cu) and bimetallic Pd–Cu catalysts were prepared by impregnation method	T=120 °C P_{H2}= 6 atm Reaction time = 2 h	Pd–Cu supported on MgO or $Mg(OH)_2$ prepared by modified electroless plating method showed the highest conversion and selectivity to furfuryl alcohol. In the furfural hydrogenation over 5%Pd–5%Cu/MgO catalyst almost

	in water as a solvent.			complete conversion and higher than 98% selectivity to furfuryl alcohol
Driscolla, O. A. et al. (2017) [41]	Studied monometallic catalysts(platinum, palladium, copper and nickel) support(SiO_2, Al-SBA-15, ß-zeolite and TiO_2) on catalysts, second metal added to platinum catalysts and varied solvent of reaction for the selective hydrogenation of furfural to furfuryl alcohol.	Monometallic catalysts were prepared by wet impregnation and bimetallic catalysts were synthesized by surface reactions using a variety of promoter metals	T=100 °C P_{H2}= 20 atm Reaction time = 5 h	- SiO_2 support catalyst showed higher furfuryl alcohol selectivity compared with all support - Pd catalysts found that showed good furfural conversion but was not selective to furfuryl alcohol. - Pt based catalysts presented high selectivity to furfuryl alcohol - Pt-Sn was the most active for the hydrogenation of furfural to furfuryl alcohol

Wang, Y. et al. (2017) [42]	Studied the CuCo-based mixed metal/metal oxide on porous carbon matrix with varied the molar ratio of cobalt to copper and calcination temperature for the hydrogenation of furfural to furfuryl alcohol	Cu/C and CuCo/C were prepared by thermal decompositio n of the Cu-BTC precursor impregnated with Co^{2+}ions.	T=140 ℃ P_{H2}= 30 atm Reaction time = 1 h	CuCo0.4/C-873 (calcination temperature = 873 K, 600℃) showed best catalytic performance with 98.7% furfural conversion and 97.7% furfuryl alcohol selectivity
Chen, B. et al. (2015) [5]	Studied the bimetallic catalysts supported over TiO_2–ZrO_2 binary oxides and used for liquid-phase hydrogenation of furfural	Ni/TiO_2-ZrO_2, Pd/TiO_2-ZrO_2 and Ni-Pd/TiO_2-ZrO_2 were prepared by co-impregnation or impregnation of metal precursors onto TiO_2-ZrO_2	T=130 ℃ P_{H2}= 50 atm Reaction time = 8 h	- The bimetallic catalyst with Ni–Pd mole ratio of 5:1 showed the best catalytic activity about yield of tetrahydrofurfuryl alcohol reaches 93.4%. - Pt–Re bimetallic catalyst especially converts furfural in to partial

				hydrogenation converted to furfuryl alcohol with 95.7% furfuryl alcohol selectivity.

Taylor, M. J. et al. (2016) [2] studied Pt nanoparticles supported on SiO_2, ZnO, ɣ-Al_2O_3, CeO_2 for selective liquid phase hydrogenation of furfural to furfuryl alcohol under extremely mild conditions and varying solvents of reaction such as polar solvent and nonpolar solvent. Pt particle size is important for furfural hydrogenation. Pt particle size is approximately 4 nm (MgO, CeO_2 and ɣ-Al_2O_3 supported Pt) is highly active and selective for the hydrogenation reaction in methanol, depending on the support of catalyst. For example, smaller Pt nanoparticles present in the MgO and SiO_2 catalysts promote some decarbonylation to furan. This reaction is also sensitive to the solvent used. They found that in alcohols solvent the reaction is more active than in non-polar solvents. Methanol and n-butanol proved to be excellent solvents for promoting high furfuryl alcohol yield. Conversely, non-polar solvents conferred poor furfural conversion, while ethanol favored acetal by-product formation.

Merlo, A. B. et al. (2009) [3] studied the effect of Sn adding on Pt/SiO_2 (varying Sn/Pt ratios) for liquid-phase hydrogenation of furfural. The Pt/SiO_2 catalyst was prepared by ion-exchange and then Sn was added by controlled surface reactions technique. The effect of solvent of reaction between nonalcoholic and non-polar solvents was investigated. Adding of Sn into Pt-based systems showed positive effect to in this reaction, in which highly selectiving to the desired product (furfuryl alcohol) was obtained. Bimetallic PtSn catalyst were more active than the monometallic catalyst. The lowest Sn/Pt atomic ratio showed highest reaction rate. When using 2-propanol as a solvent of the hydrogenation of furfural, the catalyst showed high stability. The catalyst PtSn (Sn/Pt ratio = 0.3) gave a high level of conversion after three reaction cycles.

Zhang, C. et al. (2017) [4] studied the effect of preparation of bimetallic catalyst (Ni-Pt/SiO_2 and Cu-Pt/SiO_2) and monometallic catalysts (Ni/SiO_2, Cu/SiO_2 and Pt/SiO_2) and conditions for selective hydrogenation of furfural to furfuryl alcohol. All the catalysts were prepared by directed deposition technique and compared with incipient wetness impregnation (Cu@Pt/SiO_2 and Ni@Pt/ SiO_2). Bimetallic catalyst Cu@Pt showed higher turnover frequencies of furfural hydrogenation compared to pure Pt and pure Cu. Adding Cu into Pt/SiO_2 improved reactivity which is likely to be due to fewer Pt sites being blocked by strong hydrogen adsorption as a result of decreased H_2 binding strength of Pt overlayer compared to pure Pt.

Bhogeswararao, S. et al. (2015) [1] studied the effect of temperatures of reaction of ɣ-Al_2O_3-supported Pt and Pd catalysts and concentration of metal loadings. The catalysts were prepared by wet impregnation method and tested in hydrogenation of furfural. At low temperature reaction (25℃), they found that Pt catalysts were selective for C=O hydrogenation (yielding furfuryl alcohol) but Pd catalysts hydrogenated both ring and C=O groups of furfural (producing tetrahydrofurfuryl alcohol). At higher temperatures reaction (240℃), the supported Pd catalysts enabled decarbonylation of furfural giving furan in 82% yield. At these reaction conditions, the supported Pt catalysts facilitated hydrogenolysis of C=O and C=O groups enabling 2-methylfuran and furan ring-opened products.

Musci, J. J. et al. (2017) [39] studied the effect of Sn adding in carbon-supported monometallic Ru for aqueous phase hydrogenation of furfural at 90 ℃ and 1.25 MPa. All the catalyst were prepared by impregnation method with various Sn/Ru ratios at 0, 0.1, 0.2, 0.4 and 0.8. They found that Sn/Ru ratio of 0.4 promoted the C=O hydrogenation reaching a selectivity towards furfuryl alcohol over 85% throughout the course of the reaction but when adding more Sn at higher concentration, the reaction results were not further improved. It seems to be a compromise between the dilution of Ru sites, active for the hydrogenation reaction, and the promoting effect of Sn because bimetallic RuSn/C catalysts have strong interaction between Ru and Sn.

Fulajtárova, K. et al. (2015) [40] studied the monometallic (Pd, Cu) and bimetallic Pd–Cu catalysts with different metal loadings on various supports and various preparation method of support for the selective hydrogenation of furfural to furfuryl alcohol using water as a solvent. From the results, bimetallic Pd–Cu catalysts supported on MgO and $Mg(OH)_2$ prepared by electroless plating method showed the highest conversion and selectivity to furfuryl alcohol due to both the Pd and Cu metal and the support were critical for directing the selectivity to furfuryl alcohol. They said that hydrogenated of C=O group mainly occurs on sited associated with Cu^+ ions. On these sites, the carbonyl group is polarized, facilitating hydrogen transfer from the adjacent Pd-H sites. To produce selectively furfuryl alcohol, weaker interactions between the furyl ring and surface of active metal species would be desired.

Driscolla, O. A. et al. (2017) [41] studied the monometallic catalysts (platinum, palladium, copper and nickel) on various support including (SiO_2, Al-SBA-15, β-zeolite and TiO_2), second metal added to platinum catalysts, and various solvents of reaction for the selective hydrogenation of furfural to furfuryl alcohol. Monometallic catalysts were prepared by wet impregnation and bimetallic catalysts were synthesized by surface reactions using a variety of promoter metals. For monometallic catalysts, platinum catalyst showed higher selectivity to furfuryl alcohol. In part of bimetallic catalysts, they found that second metal affected the conversion of furfural followed the order of tin > molybdenum > manganese > barium > iron > nickel. All bimetallic catalysts showed 100% selectivity of furfuryl alcohol.

Wang, Y. et al. (2017) [42] studied the CuCo-based mixed metal/metal oxide on porous carbon matrix with various the molar ratios of cobalt to copper and calcination temperatures for the hydrogenation of furfural to furfuryl alcohol. They found that CuCo0.4/C-873 (Co/Cu molar ration = 0.4 and calcination temperature = 873 K) showed best catalytic performance with 98.7% fufural conversion and 97.7% furfuryl alcohol selectivity in medium polar solvent at 413 K and 3 MPa hydrogen pressure maybe due to particle size influence to catalytic performance that small particle size (about 9 nm) showed good catalytic performance and the synergistic effect

of copper and cobalt and also showed good stability in recycling test. High surface area and porosity alsoled to high conversion and selectivity.

Chen, B. et al. (2015) [5] studied the bimetallic catalysts supported on TiO_2–ZrO_2 binary oxides prepared by co-impregnation methods and used for liquid-phase hydrogenation of furfural. Bimetallic synergistic effect influenced to highly selective hydrogenation Ni-Pd catalyst with mole ratio of 5:1 shows the best performance for total hydrogenation to tetrahydrofurfuryl alcohol (THFA). The yield of THFA reaches 93.4% due to synergistic effect of Ni-Pd, which is interpreted through XPS measurement and a hydrogen-transfer mechanism is proposed. Pt–Re bimetallic catalyst is an excellent partial hydrogenation catalyst selective to furfuryl alcohol (FA)(yield of FA reaches 95.7%) because rheniumoxide species was located on the Pt surface, the hydrogen species on Pt are transferred to adsorbed C=O bond to achieve selective hydrogenation.

CHARPTER III

MATERIALS AND METHODS

This chapter explains the detail of experimental of this research in four parts including materials, catalyst preparation, catalyst characterization and evaluation of catalytic performance in selective hydrogenation of furfural. Catalyst preparations are flame spray pyrolysis and impregnation methods. Catalyst characterization techniques are as N_2 physisorption, X-ray diffraction (XRD), CO pulse chemisorption, H_2-temperature programmed reduction (H_2-TPR), Atomic absorption spectroscopy (AAS), transmission electron spectroscopy (TEM), and X-ray photoelectron spectroscopy (XPS).

3.1 Materials

Table 3 shows the chemicals used as precursors for catalyst preparation (impregnation and flame spray pyrolysis methods) and reaction study in this research.

Table 3.1 Chemicals used in catalyst preparation and reaction study

Order	Chemicals	Formula	Suppliers
1	Platinum(II)acetyl-acetonate 99.99%	$Pt(C_5H_7O_2)_2$	Aldrich
2	Cobalt naphthenate, 6 wt% in mineral spirits	$CoC_{22}H_{14}O_4$	Aldrich
3	Titanium(IV) butoxide reagent grade, 97%	$Ti(OCH_2CH_2CH_2CH_3)_4$	Aldrich
4	Xylene 99.8%	C_8H_{10}	Merck

5	Furfural 99%	$C_5H_4O_2$	Aldrich
6	Furfuryl alcohol 99%	$C_5H_6O_2$	Aldrich
7	Tetrahydrofurfuryl alcohol 98%	$C_5H_{10}O_2$	Aldrich
8	Furan 98%	C_4H_4O	Aldrich
9	Methanol 98%	CH_3OH	Aldrich

3.2 Catalyst preparation

3.2.1 Preparation of monometallic Pt /TiO_2 catalyst by flame spray pyrolysis method

The monometallic Pt/TiO_2 (0.5 wt% Pt) was prepared by FSP method according to the procedure reported in Ref.[11]. Platinum actetylacetonate and titanium (IV) butoxide reagent were used as platinum and titanium precursors, respectively. The designed amounts of metal precursor in xylene (MERCK; 99.8 vol.%) were prepared with total metal concentration at 0.3 M and fixed concentration of Pt at 0.5 wt%. Liquid precursor solution was then fed into flame reactor by a syringe pump at 5 mL/min and dispersed with oxygen 5 L/min forming a fine droplets by a gas- assisted nozzle fed by 5 L/min of oxygen (Thai Industrial Gas Limited; purity >99%). Pressure drop (capillary tip) was maintained at 1.5 bar, the orifice gap area at nozzle was adjusted. The spray was burned by supporting flame lets fed with oxygen (3 L/min) and methane (1.5 L/min) which were positioned in a ring around the nozzle outlet. A sintered metal plate ring (8 mm wide, starting at a radius of 8 mm) provided an additional 10 L/min of oxygen as sheath for the supporting flame. The product particles were produced by passing through the flame at a temperature of approximately 2000°C in milliseconds and collected on a glass fiber filter (Whatman GF/C, 15 cm in diameter) with the aid of a vacuum pump shown in Figure 3.1

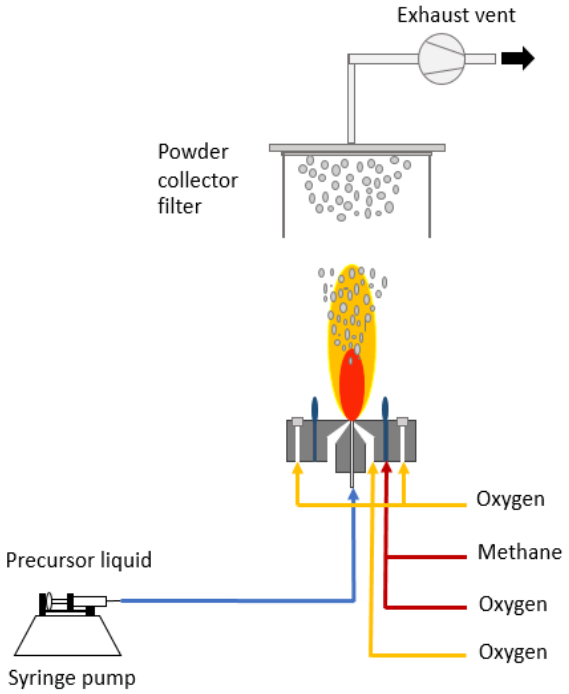

Figure 3.1 Diagram of flame spray pyrolysis

3.2.2 Preparation of monometallic Pt/TiO_2 catalysts by impregnation method.

The Pt/TiO_2 (0.5 wt% Pt) catalysts were prepared by impregnation method. Platinum actetylacetonate was dissolved in xylene and dropped into titanium (P25) support. Then the catalysts were dried in room temperature for 6 h and dried in an oven at 100°C overnight in air. Afterwards, the catalysts were calcined in air at 500°C for 2 h. Finally the catalysts were reduced in H_2 flow (25cm^3/min) at 500 °C for 2 h shown in Figure 3.2

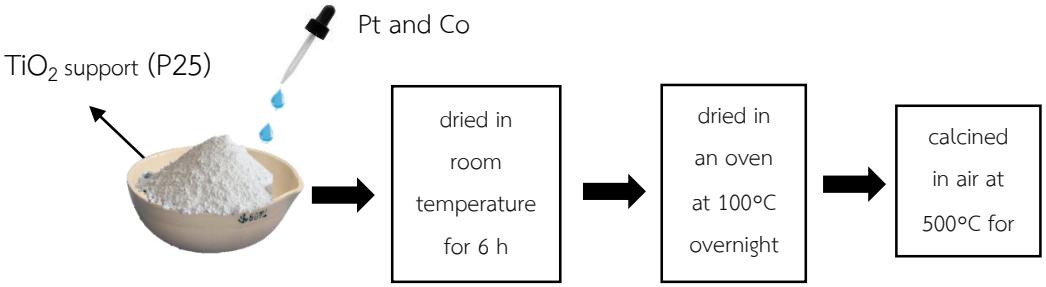

Figure 3.2 Diagram of Pt/TiO_2 and PtCo/TiO_2 catalysts preparation by impregnation method

3.2.3 Preparation of bimetallic $PtCo/TiO_2$ catalysts by flame spray pyrolysis method

Synthesize of bimetallic catalysts(0.5 wt% Pt and varying %Co loading at 0-0.8 wt.% Co) were carried out using a spray flame reactor similar to that of Ref.[11]. For PtCo/TiO2 catalysts, platinum actetylacetonate, cobalt naphthenate 10 wt% in mineral spirits, and titanium (IV) butoxide were used as platinum, cobalt, and titanium precursors, respectively. Precursors were prepared by dissolving the designed amounts of metal precursor in xylene (MERCK; 99.8 vol %). Total metal concentration at 0.3 M fixed concentration of Pt at 0.5 wt%. Liquid precursor solution was then fed into flame reactor by a syringe pump at 5 mL/min and dispersed with oxygen 5 L/min forming a fine droplets by a gas- assisted nozzle fed by 5 L/min of oxygen (Thai Industrial Gas Limited; purity >99%). Pressure drop (capillary tip) was maintained at 1.5 bar, the orifice gap area at nozzle was adjusted. The spray was burned by supporting flame lets fed with oxygen (3 L/min) and methane (1.5 L/min) which were positioned in a ring around the nozzle outlet. A sintered metal plate ring (8 mm wide, starting at a radius of 8 mm) provided an additional 10 L/min of oxygen as sheath for the supporting flame. The product particles were produced by passing through the flame at a temperature of approximately 2000°C in milliseconds and collected on a glass fiber filter (Whatman GF/C, 15 cm in diameter) with the aid of a vacuum pump shown in Figure 3.1

3.2.4 Preparation of bimetallic $PtCo/TiO_2$ catalysts by co-impregnation method.

The $PtCo/TiO_2$ (0.5 wt% Pt and varying %Co loading at 0-0.2 wt.% Co) catalysts were prepared by co-impregnation method. . Platinum actetylacetonate and cobalt naphthenate were dissolved in xylene and dropped into titanium (P25) support. Then the catalysts were dried in room temperature for 6 h and dried in an oven at 100°C overnight in air. Afterwards, the catalysts were calcined in air at 500°C for 2 h. Finally the catalysts were reduced in H_2 flow (25cm^3/min) at 500 °C for 2 h shown in Figure 3.2

3.3 Catalyst characterization

To investigate the physiochemical properties of catalysts, fresh catalysts was characterized by several techniques.

3.3.1 X-ray diffraction (XRD)

XRD patterns were determined using a Bruker D8 Advance using nickel filtered CuK_{α} radiation. The crystallite size (d_{XRD}) was calculate using the Scherrer's equation and α-alumina as the external standard.

3.3.2 N_2-physisorption

The BET surface area, average pore size diameters, and pore size distribution were determined by using nitrogen adsorption in a Micrometrics ASAP 2020 instrument.

3.3.3 Atomic absorption spectroscopy (AAS)

The amount of actual Pt and Co loading in catalysts were measured from atomic absorption spectroscopy technique. A spectroanalytical procedure for the quantitative determination of chemical elements using the absorption of optical radiation (light) by free atoms in the gaseous state.

3.3.4 H_2-Temperature programmed reduction (H_2-TPR)

The H_2-TPR experiments were performed to determine reducibility and reduction temperature of platinum catalysts. The demonstration were carried out in a quartz U-tube reactor. For each measurements, all the catalyst samples were pretreated with a N_2 flow (25 cm^3/min, 1 h, 150°C). The TPR profiles were obtained by passing carrier gas (10% H_2 in nitrogen) through the catalyst samples (30 mL/min) with a temperature ramp from room temperature to 600 °C at 10°c/min.

3.3.5 Transmission electron spectroscopy (TEM)

The morphology and crystallite sizes of monometallic catalysts (Pt/TiO_2) and bimetallic catalysts ($PtCo/TiO_2$) were measured by using JEOL-JEM 2010 transmission electron microscope using energy-dispersive X-ray detector operated at 200 kV.

3.3.6 X-ray photoelectron spectroscopy (XPS)

The XPS spectra, the blinding energy, full width at half maximum (FWHM) and the composition of the Pt catalysts on the surface layer of the catalysts were performed by using the Kratos Amicus x-ray photoelectron spectroscopy. The experiment was operated with the x-ray source at 20 mA and 12 kV (240 W), the resolution at 0.1 eV/step and the pass energy of the analyzer was set at 75 eV under pressure approximately 1x10-6 Pa. For calibration, the blinding energy was referenced to C 1s line at 285.0 eV. The blinding energy of O 1s, Ti 2p and Pt 4f are determined.

3.3.7 CO pulse chemisorption

The percentages of platinum dispersion were measured from CO-pulse chemisorption technique using a Micromeritics ChemiSorb 2750 (pulse chemisorption system). About 0.05 g. of catalyst was reduced under hydrogen flow (25 cm^3/min) at 500 °C for 2 h with a heating rate of 10°c/min and cooled down to the room temperature, and then helium gas was inserted into the sample cell (25 cm^3/min) for remove air. The CO was pulsed over the reduced catalyst until the TCD signal from the pulse was constant. Next, 20 μL of carbon monoxide was injected into catalysts and repeated until the desorption peak were unchanged.

3.4 Evaluation of catalytic performance in selective hydrogenation of furfural

The catalytic performances of the prepared catalysts were tested in the liquid phase selective hydrogenation of furfural to FA. Approximately 0.05 g of catalyst, 50 μL of furfural and 10.0 mL methanol of were loaded into in a 100 mL stainless steel autoclave reactor (JASCO, Tokyo, Japan). The reactor was purged with hydrogen to remove the air for three times. The reaction was executed at 50 °C, 2 MPa of H_2 for 120 min. The reaction was controlled while stirring the reaction mixture with a magnetic stirrer. After the reaction, the reactor was cooled to below room temperature with an ice-water and carefully depressurized. The liquid product was then analyzed by a gas chromatograph attached with a flame ionization detector.

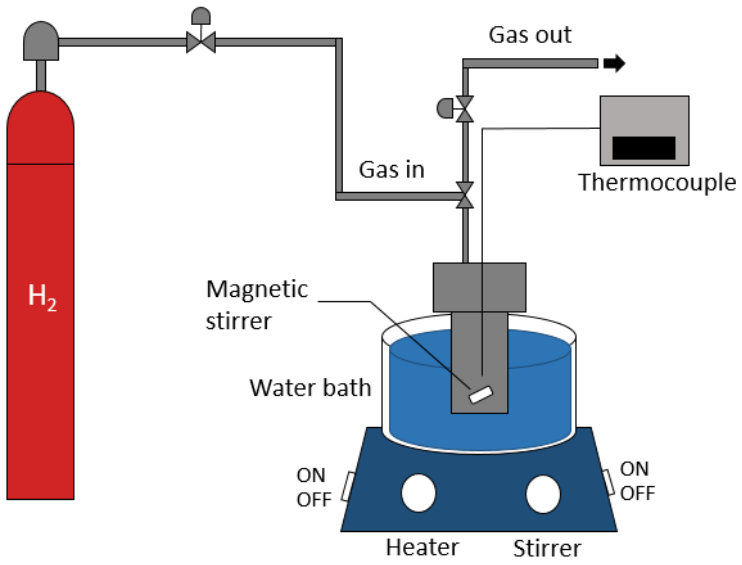

Figure 3.3 Schematic of the liquid-phase hydrogenation of furfural.

Table 3.2 Gas-Chromatography operating conditions

Gas chromatography (Shimadzu GC-2014)	Conditions
Detector	FID
Packed column	Rtx®5
Carrier gas	Helium (99.99 vol.%)
Make-up gas	Air (99.9 vol.%)
Column temperature	110 °C
Injector temperature	260 °C
Detector temperature	270 °C
Time analysis	41.80 min

CHARPTER IV
RESULTS AND DISCUSSION

This chapter discusses about the physiochemical and catalytic properties of Pt/TiO_2 and $Pt\text{-}Co/TiO_2$ prepared by flame spray pyrolysis and impregnation method. The results and discussion is divided into two major parts. In the first part, the influence of Co loading on Pt/TiO_2 catalyst synthesized by impregnation method for liquid selective hydrogenation of furfural was reported. And in the second part, the influence of Co loading on Pt/TiO_2 catalyst synthesized by flame spray pyrolysis for liquid selective hydrogenation of furfural was reported and compared with the ones prepared impregnation method.

4.1 Influence of Co loading on Pt/TiO_2 catalyst synthesized by impregnation method for the liquid-phase selective hydrogenation of furfural

The aims of this section were to investigate the properties of impregnated monometallic Pt/TiO_2 and bimetallic $PtCo/TiO_2$ catalysts in the selective hydrogenation of furfural. The catalytic performances were correlated with the physicochemical properties of the catalysts obtained by various characterization techniques such as X-ray diffraction (XRD), N_2-physisorption, H_2-temperature programmed reduction (H_2-TPR), transmission electron spectroscopy (TEM), X-ray photoelectron spectroscopy (XPS), atomic absorption spectroscopy and CO pulse chemisorption.

The Pt/TiO_2 catalyst prepared by impregnation was referred to as (I)-Pt/TiO_2 and the bimetallic catalysts, the $Pt\text{-}Co/TiO_2$ catalyst synthesized by impregnation method was referred to as (I) $Pt\text{-}Co/TiO_2$. The synthesized bimetallic particles were denoted as I - XCo/TiO_2 where X is Co loading contents in wt%.

4.1.1 X-ray diffraction (XRD)

The XRD patterns of monometallic and bimetallic catalysts synthesized by impregnation method are shown in Figure 4.1. Both monometallic and bimetallic catalysts exhibited the characteristic peaks of anatase TiO_2 at 2θ = 25° (major), 37°, 48°, 55°, 56°, 62°, 71°, and 75° and rutile phase at 2θ = 28° (major), 36°, 42°, and 57° [43]. The characteristic peaks of platinum and cobalt species were not detected for all the catalysts due to low amount of metals present and/or high dispersion of these metals on the TiO_2 supports. The average crystallite sizes of anatase phase TiO_2 support were calculated by the Scherre's equation from the full width at half maximum of the XRD peak at 2θ=25°. The average crystallite size of anatase phase TiO_2 supports and %anatase phase of the TiO_2 support of both synthesis catalysts are summarized in Table 4.1.

For monometallic Pt/TiO_2 catalysts, the average crystallite size of the anatase phase TiO_2 was approximately 12 nm with %anatase phase at 85.8 %. The impregnation of Pt precursor onto TiO_2 support (P25) resulted in the decrease of %anatase phase from 91.3 to 85.8%. However, Co addition as a second metal into Pt/TiO_2 catalysts was found to prevent the anatase to rutile transformation as seen in the (I) $Pt\text{-}0.2Co/TiO_2$ catalyst. It has been suggested that the Co^{2+} can enter in anatase structure since ionic radius of Co^{2+} (0.075 nm) is similar to Ti^{4+} (0.061 nm) [44]. The entering of cationic dopant in this case may decrease the level of oxygen vacancies, thereby inhibiting anatase to rutile transformation [45, 46]. However, CO addition at 0.4wt% resulted in the decrease of %anatase phase from 91.3 to 87.6%. This observation might be due to the formation of Co new phase; nevertheless, this phase could not be detected in the XRD results because of low amount of Co addition. There was little influence of Co addition on the average crystallite size of anatase phase TiO_2,which was determined to be in the range of approximately 12-15 nm.

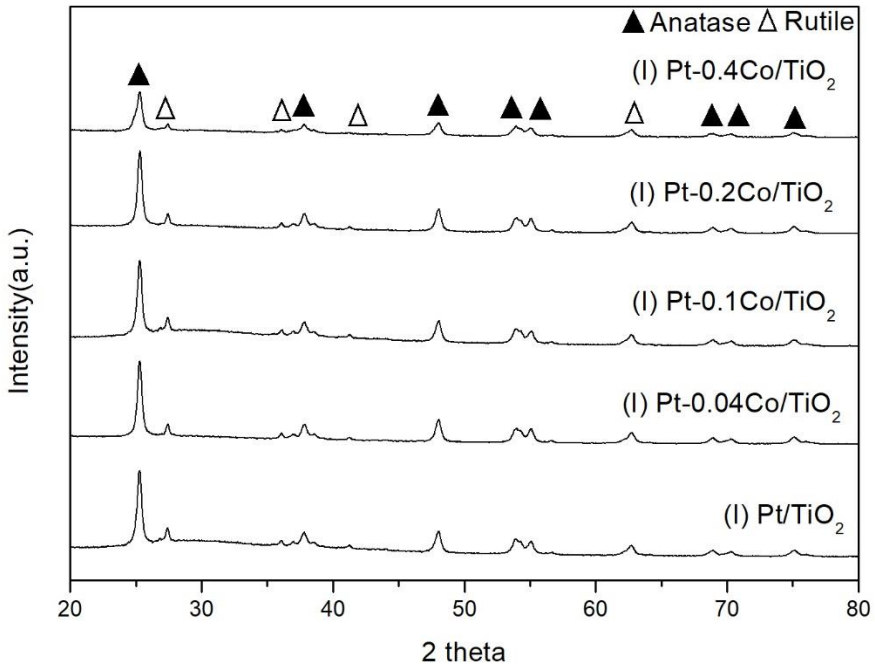

Figure 4.1 The XRD patterns of (I) Pt/TiO_2 and (I) $Pt-Co/TiO_2$ catalysts

4.1.2 N_2-physisorption

The BET surface area, pore volume, average pore diameter, and N_2 adsorption-desorption isotherms were determined by N_2-physisorption. The BET surface area, pore volume, and pore diameter of the Pt/TiO_2 and $Pt-Co/TiO_2$ catalysts prepared by impregnation method are shown in Table 4.1. The N_2 adsorption-desorption isotherms of the Pt/TiO_2 and $Pt-Co/TiO_2$ catalysts prepared by impregnation method are shown in Figure 4.2.

The monometallic Pt/TiO_2 showed BET surface area, pore volume, and average pore diameter at 52.2 m^2/g, 16.5 nm and 0.28 cm^3 (STP)/g, respectively. For bimetallic catalysts, Co adding slightly affected BET surface area, pore volume, and average pore diameter. The BET surface area, average pore volume, and pore diameter of the (I) Pt/TiO_2 and (I) $Pt-Co/TiO_2$ were almost the same at around 52.2 to 60 m^2/g, 0.28 to 0.44 cm^3/g and 16.5 to 25.1 nm, respectively. From the N_2 adsorption-desorption isotherms results, both Pt/TiO_2 and $Pt-Co/TiO_2$ catalysts prepared by impregnation method exhibited type IV physisorption isotherm with hysteresis loop, corresponding

the characteristic of mesoporous materials with pore diameters between 2 and 50 nm. The hysteresis loop type H3 indicated the slit shaped pores and/or panel-shaped particles.

Table 4.1 Physical properties of (I) Pt/TiO_2 and (I) $Pt\text{-}Co/TiO_2$catalysts

Catalyst	Crystallite size of anatase TiO_2[a] (nm)	%Phase composition[a]		BET surface areas (m^2/g)	Average pore diameter[b] (nm)	Pore volume[b] (cm^3(STP)/g)
		Anatase	Rutile			
P25	-	91.3	8.7	-	-	-
(I) Pt/TiO_2	12.0	85.8	14.2	52.2	16.5	0.28
(I) Pt-0.04Co/ TiO_2	14.0	88.1	11.9	59.3	18.7	0.34
(I) Pt-0.1Co/TiO_2	14.3	89.7	10.3	59.5	18.8	0.35
(I) Pt-0.2Co/TiO_2	15.5	90.5	9.5	60.0	25.1	0.44
(I) Pt-0.4Co/TiO_2	11.9	87.6	12.4	55.6	23.7	0.38

[a] Base on the XRD results

[b] Determined from the Barret-Joyner-Halenda(BJH) desorption method

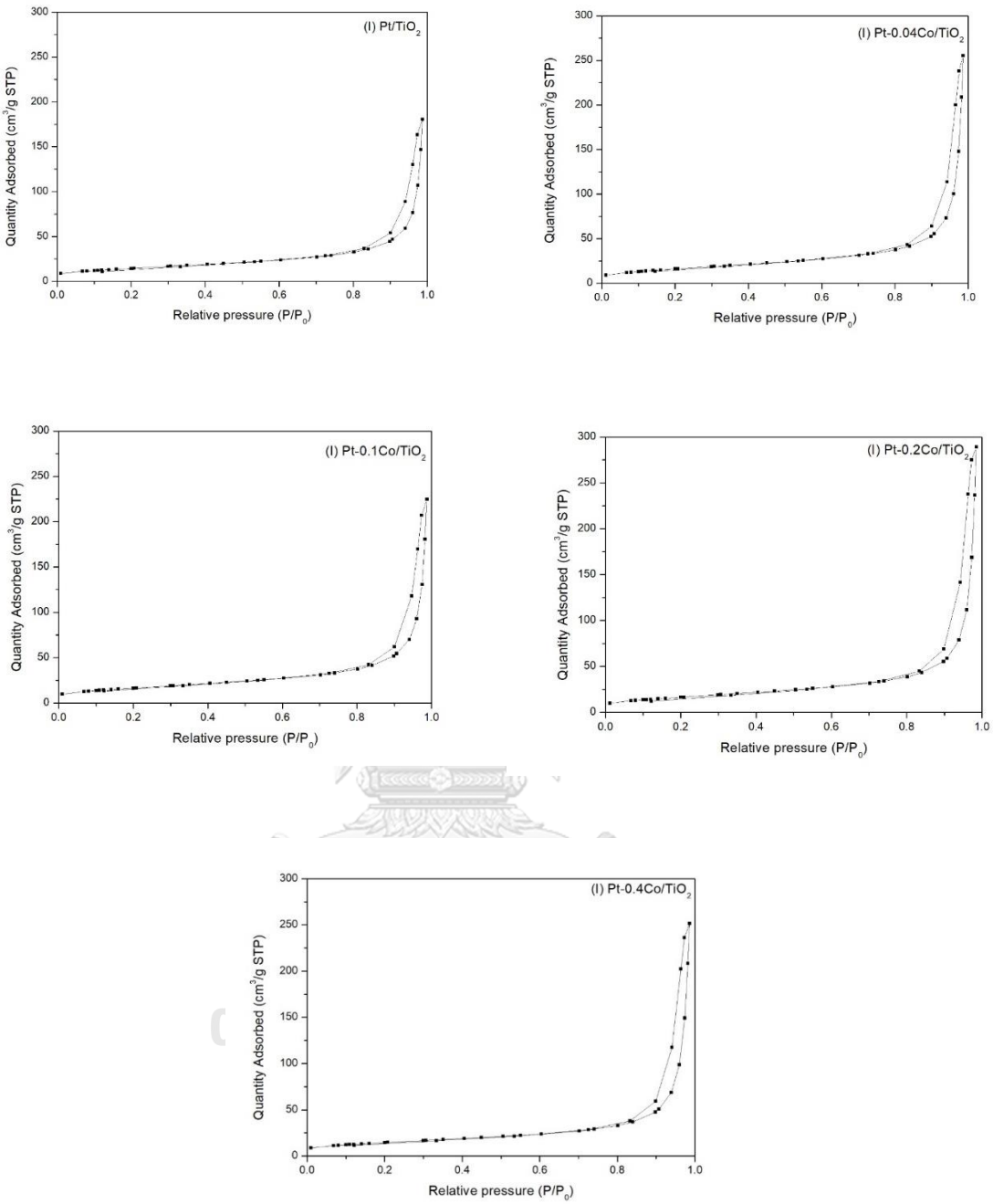

Figure 4.2 The N_2 adsorption-desorption isotherms of (I) Pt/TiO_2 and (I) $Pt\text{-}Co/TiO_2$ catalysts

4.1.3 H_2-Temperature programmed reduction (H_2-TPR)

The reduction behaviors of the monometallic Pt/TiO_2 and bimetallic Pt-Co/TiO_2 catalysts prepared by impregnation method were studied by H_2-TPR technique. The results are shown in Figure 4.4. Both monometallic and bimetallic catalysts showed three reduction peaks at 94-100 °C, 321-331 °C, and 509-545 °C. The first reduction peak was correlated to the reduction of PtO_x to metallic Pt^0 [23, 47]. The second reduction peak was associated to reduction of Pt species interacting with the TiO_2 support to form Pt-TiO_x interface site[23, 48] and third reduction peak was the hydrogen consumption above 500 °C due to the reduction of surface capping oxygen of TiO_2 [23].

Co addition into Pt based catalyst slightly altered the H_2-TPR profiles of the catalysts. The first reduction peaks of impregnated catalysts were similar to monometallic Pt/TiO_2 catalyst. The second reduction peaks were shifted to higher reduction temperatures when Co was added to the Pt/TiO_2 catalysts, suggesting stronger interaction between metal and TiO_2 support. It is also possible that some cobalt particles migrated onto the Pt surface [7]. In addition, the third reduction peaks were found to be shifted to higher reduction temperatures upon the Co addition as the second metal, suggesting that TiO_2 was more difficult to reduce. Additionally, the second reduction peak of (I) Pt-0.4Co/TiO_2 catalyst appeared as flat peak due to lower amount of Pt-TiO_x and Co-PtTiO_x species.

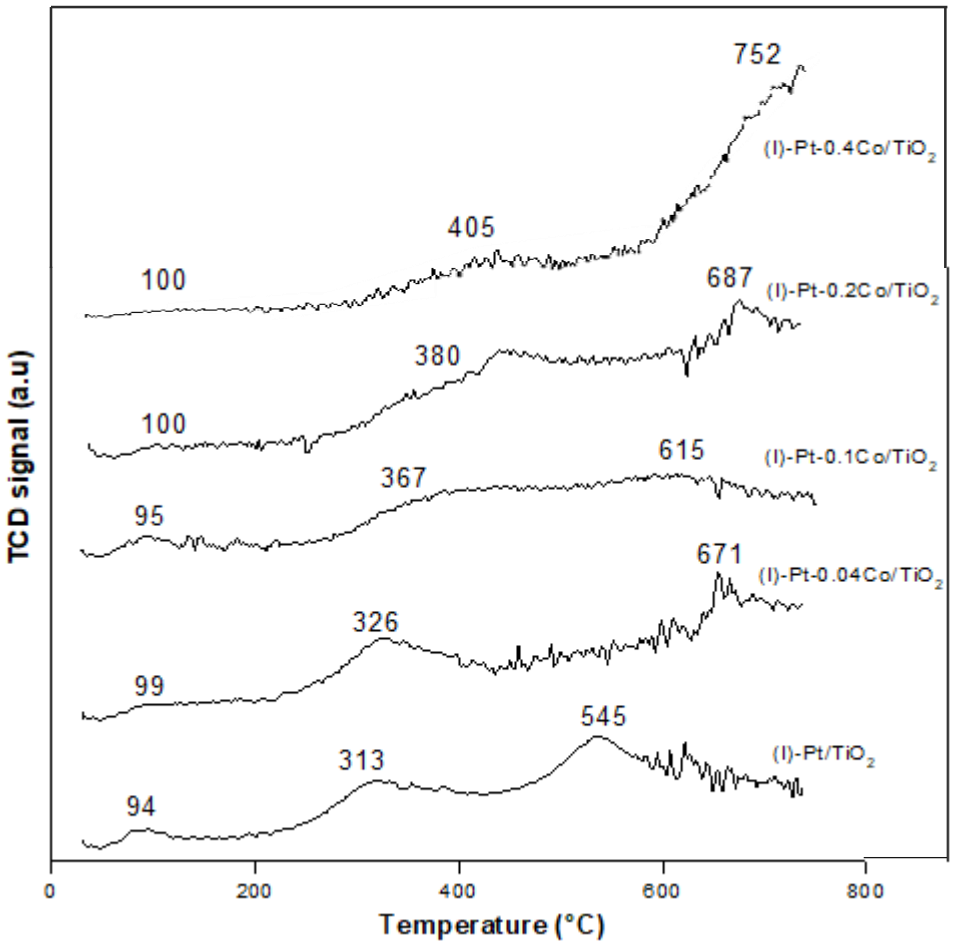

Figure 4.3 H_2-TPR profiles of (I) Pt/TiO_2 and (I) $Pt\text{-}Co/TiO_2$ catalysts

4.1.4 Transmission electron spectroscopy (TEM)

The morphology and metal particles size of catalysts can be found from TEM analysis. The TEM images of (I) Pt/TiO_2, (I) $Pt\text{-}0.2Co/TiO_2$ and (I) $Pt\text{-}0.4Co/TiO_2$ catalysts are shown in Figure 4.5-4.7, respectively.

From the TEM results, monometallic Pt/TiO_2 catalyst showed metal particles size at 8.9 nm. Upon Co addition into monometallic Pt/TiO_2 catalyst, the metal particle sizes were found to decrease from 8.9, 4.0 and 3.5 nm for Co loading contents increased from 0, 0.2, and 0.4 wt%, respectively. The $Pt\text{-}Co/TiO_2$ catalyst indicated stronger interaction between metal and TiO_2 support than Pt/TiO_2 catalyst therefore higher resistance to surface migration of metal particles, affecting to the decrease in

metal particles size [49]. These results were consistent with the H_2-TPR observation. Considering the EDX results (result not shown), the %weight of Pt/Ti ratios for (I) Pt-0.2Co/TiO_2 and (I) Pt-0.4Co/TiO_2 catalyst were 0.022% and 0.012%, respectively.

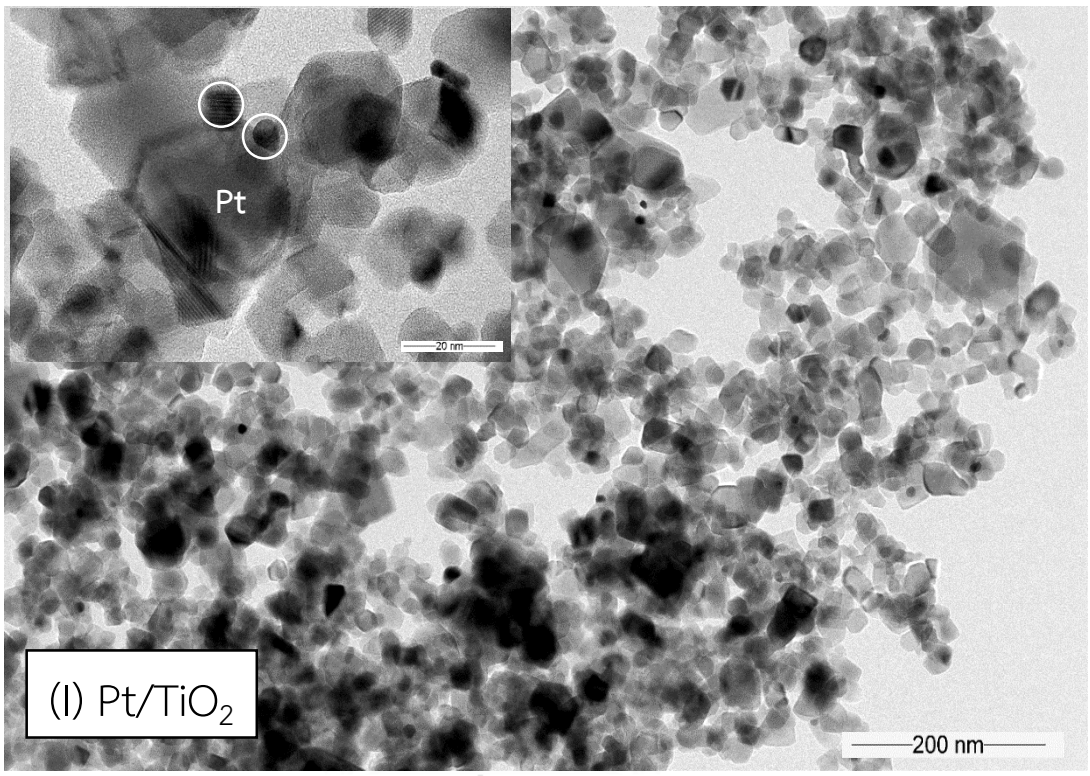

Figure 4.4 TEM images of the (I) Pt/TiO_2 catalyst

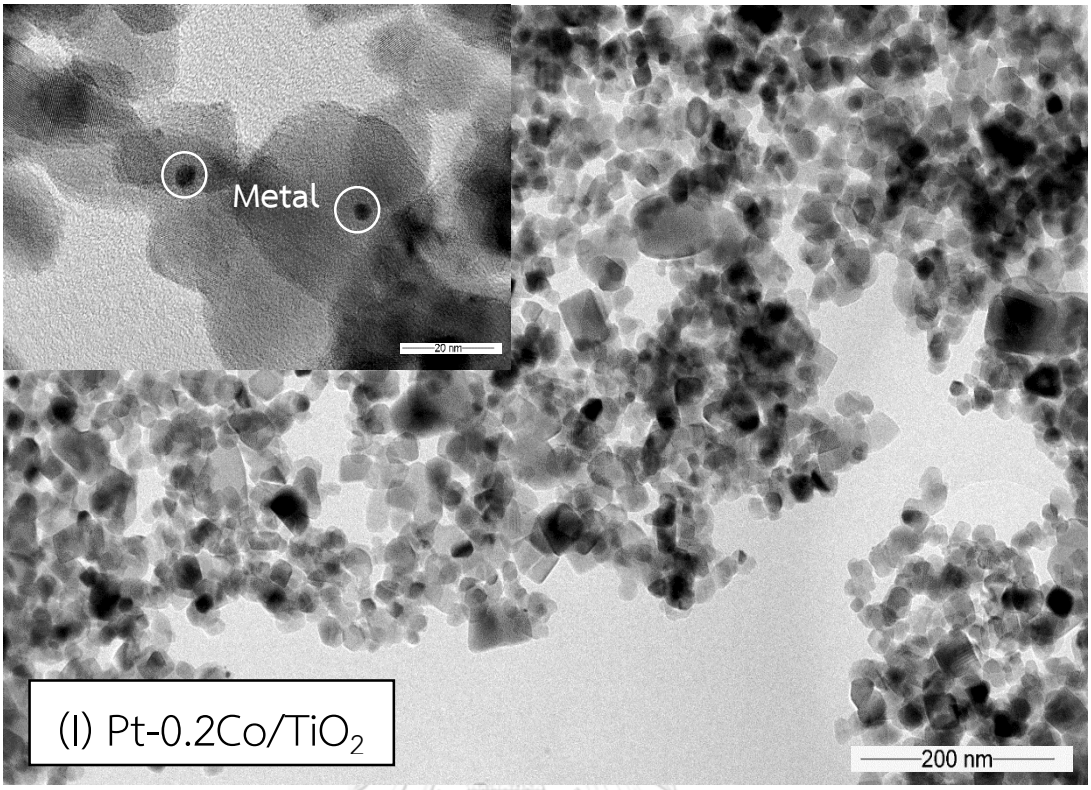

Figure 4.5 TEM images of the (I) Pt-0.2Co/TiO_2 catalyst

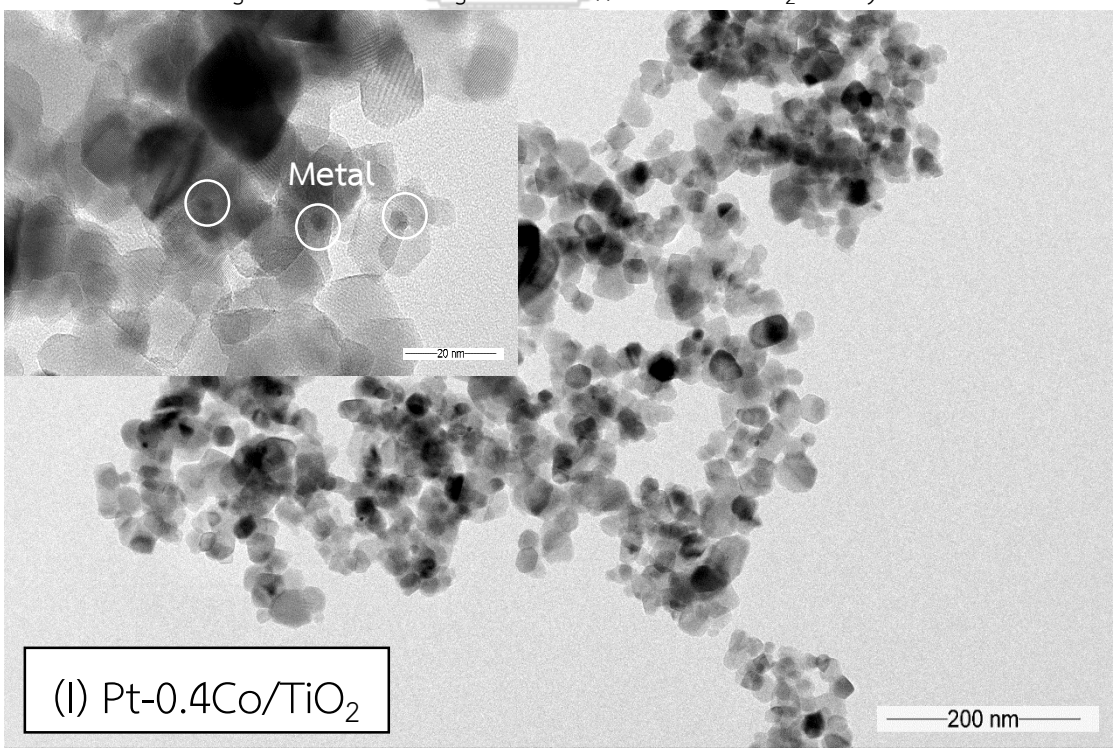

Figure 4.6 TEM images of the (I) Pt-0.4Co/TiO_2 catalyst

4.1.5 X-ray photoelectron spectroscopy (XPS)

X-ray photoelectron spectroscopy (XPS) is a technique that use to confirm the presence of element. The XPS spectra of Ti 2p, the XPS spectra of Ti 2p of Pt/TiO_2, and $Pt\text{-}0.2Co/TiO_2$ catalysts prepared by impregnation method are shown in Figure 4.7. There were two peaks at around 458.9 eV and 464.6 eV, which corresponded to the $Ti2p_{3/2}$ and $Ti2p_{1/2}$, respectively[50]. These values were corresponding to the Ti^{4+}.

From the XPS results, the monometallic Pt/TiO_2 and bimetallic $Pt\text{-}0.2Co/TiO_2$ catalysts exhibited similar position of $Ti2p_{3/2}$ and $Ti2p_{1/2}$ peaks.

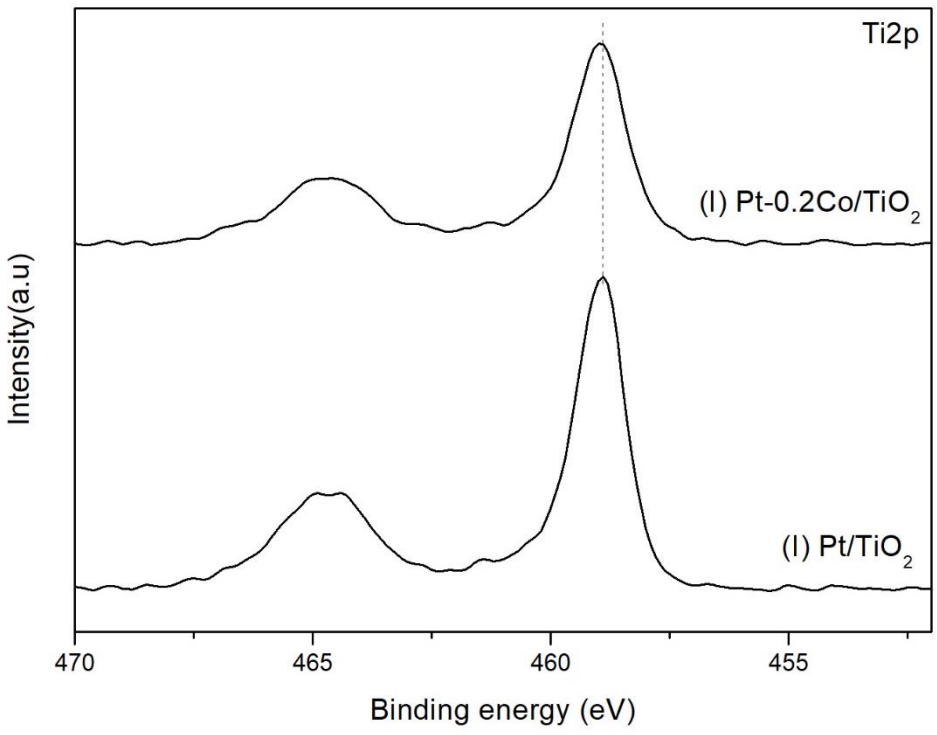

Figure 4.7 The XPS spectra of Ti 2p, the XPS spectra of Ti 2p of (I) Pt/TiO_2 and (I) $Pt\text{-}0.2Co/TiO_2$ catalysts

4.1.6 CO pulse chemisorption

The amounts of active Pt sites and %Pt dispersion on the catalyst samples were estimated from CO chemisorption. All the catalysts were reduced under H_2 flow at 500 °C before CO injection to adsorb on active sites. The %Pt dispersion were determined based on the assumption that one molecule of CO adsorbed on one molecule of Pt and none of CO molecule adsorbed on Co sites. Our research group tested Co/TiO_2 catalyst by CO chemisorption and found that very little CO adsorbed on Co/TiO_2. The % Pt dispersion and amount of active sites of Pt/TiO_2 and Pt/Co-modified TiO_2 of impregnated catalysts are shown in Table 4.2.

Considering Co addition into (I) Pt/TiO_2 catalyst, it was found that addition of Co into the Pt/TiO_2 catalysts resulted in increased percentages of platinum dispersion. Similar results have been reported by Lu, G. et al.[51] for the synthesized Pt-Co/NaY by ion exchange of NaY zeolite. They found that addition of Co enhanced CO adsorbed on catalyst because of 2 possible reasons. First, platinum surface was modified by Co and subsequently form bimetallic particles. Pt metal particles of monometallic catalyst in the zeolite are electron deficient affecting to low CO adsorbed. Adding Co resulted in an interaction between cobalt and platinum, hence it will compensate the deficiency by rehybridization of the d-electrons and CO adsorption is enhanced with increasing cobalt mole fraction. For the second reason, addition of Co led to sandwich structure formation which outer layer is pure Pt and inner layer is Co and when cobalt fraction increases. It will made either the surface composition of the bimetallic particles change or the platinum properties are further modified by cobalt in the sublayer.

Table 4.2 CO chemisorption results of (I) Pt/TiO_2 and (I) $Pt\text{-}Co/TiO_2$ catalysts

Catalyst	Pt actual loading[a] (wt%)	Co actual loading[a] (wt%)	Amount of active sites ($x10^{18}$) ($x10^{18}$molecule CO/g cat)	%Pt dispersion[b]
(I) Pt/TiO_2	0.73	-	4.7	23.4
(I) $Pt\text{-}0.04Co/TiO_2$	0.70	0.04	4.8	26.8
(I) $Pt\text{-}0.1Co/TiO_2$	0.67	0.11	5.8	32.2
(I) $Pt\text{-}0.2Co/TiO_2$	0.66	0.22	5.8	35.0
(I) $Pt\text{-}0.4Co/TiO_2$	0.60	0.39	5.8	38.1

[a] Results from Atomic absorption spectroscopy

[b] Calculations based on Pt actual loading from atomic absorption spectroscopy

4.1.7 Evaluation of the catalyst performance in the selective furfural hydrogenation

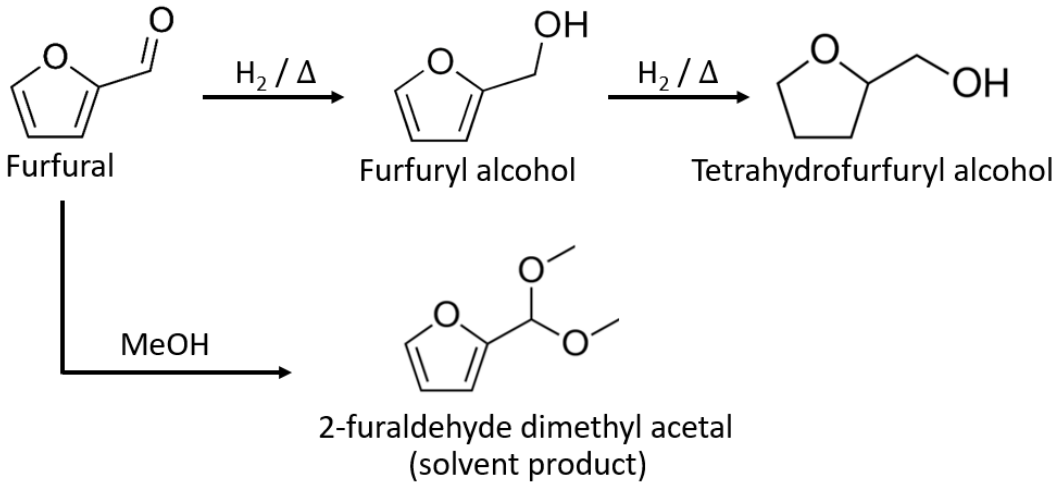

Figure 4.7 Simplified reaction scheme of the hydrogenation of furfural

Simplified mechanism of selective furfural hydrogenation are shown in Figure 4.11, Furfural is hydrogenated at C=O bond transformed to furfuryl alcohol (FA) and after that FA is hydrogenated at both C=C bond transformed to tetrahydrofurfuryl alcohol, However when using methanol as a solvent, 2-furaldehyde dimethyl acetal (solvent product, labeled as SP) may be formed [2]. The desire product in this reaction is FA. The performances of monometallic and bimetallic catalysts prepared by impregnation method were investigated in the selective furfural hydrogenation under the following reaction conditions: 50 °C, 2 MPa of H_2, methanol as a solvent. The results of selective furfural hydrogenation of monometallic Pt/TiO_2 and bimetallic Pt-Co/TiO_2 catalysts synthesized by impregnation method including furfural conversion and product selectivity are summarized in Table 4.4.

The monometallic Pt/TiO_2 catalyst exhibited furfural conversion and FA selectivity at 84.6% and 71.5%, respectively. When Co was added into monometallic impregnated Pt/TiO_2 catalysts up to 0.2wt%Co, both furfural conversion and FA selectivity were increased because Co adding into impregnated Pt/TiO_2 catalysts affected the reduction behavior of the catalysts. The second reduction peak were shifted to higher temperature and both % Pt dispersion and %anatase phase of TiO_2 support were incresed. Because the second reduction peak were shifted to higher temperature, it indicates a stronger interaction between Pt and TiO_2 support to form Pt-TiOx interface sites that could increase FA selectivity. Similar results were reported by Dandekar, A. et al[52] that special sites created at the metal–TiO_2 interface by TiO_x entities which can migrate and decorate the Pt particles enhanced carbonyl bond hydrogenation. The Ti^{3+} or Ti^{2+} cations in these suboxide species can interact with the terminal oxygen in crotonaldehyde to activate the C=O bond. In this work, an increase of furfural conversion may be related to increasing of %anatase phase when Co adding into impregnated Pt/TiO_2 catalyst because oxygen vacancies from reduced metal-anatase TiO_2 support are favorable adsorption sites for hydrogen atoms [53] while molecular hydrogen weakly interact with metal-rutile TiO_2 surface [54]. However, increasing Co addition up to 0.4 wt.%, both furfural conversion and FA selectivity was

dramatically decreased as compared to (I) Pt-0.2Co/TiO_2 catalyst. The decrease in furfural conversion and FA selectivity was due to lower Pt/Ti ratio and the lowest amount of Pt-TiO_x and Co-PtTiO_x species, respectively.

Table 4.3 The reaction results of (I) Pt/TiO_2 and (I) Pt-Co/TiO_2 catalysts

Catalyst	%Conversion	%Selectivity		%Yield of FA
		FA	SP	
(I) Pt/TiO_2	84.6	71.5	28.5	60.5
(I) Pt-0.04Co/TiO_2	85.8	88.9	11.1	76.3
(I) Pt-0.1Co/TiO_2	86.4	93.5	6.5	80.8
(I) Pt-0.2Co/TiO_2	100	97.5	2.5	97.5
(I) Pt-0.4Co/ TiO_2	45.1	49.8	50.2	22.5

Reaction (50 µL furfural in 10 ml methanol) at 50 °c with a 50 mg catalyst under 20 bar H_2 after 120 min

FA = Furfuryl alcohol

SP = Solvent product

4.2 Influence of Co loading on Pt/TiO_2 catalyst synthesized by flame spray pyrolysis for the liquid-phase selective hydrogenation of furfural and comparison with impregnation method.

From part 4.1 results, it was found that the bimetallic (I) $Pt\text{-}0.2Co/TiO_2$ catalyst showed the best catalytic performance so this Co ratio was chosen to prepare the $Pt\text{-}Co/TiO_2$ catalysts by flame spray pyrolysis for comparison with $Pt\text{-}0.2Co/TiO_2$ prepared by impregnation method. The effect of cobalt loading on Pt/TiO_2 catalyst synthesized by flame spray pyrolysis was also investigated.

The effect of Co loading on Pt/TiO_2 catalyst synthesized by flame spray pyrolysis for the liquid-phase selective hydrogenation of furfural and comparison with impregnation method were investigated and discussed in this section by means of several characterization techniques such as X-ray diffraction (XRD), N_2-physisorption, H_2-temperature programmed reduction (H_2-TPR), transmission electron spectroscopy (TEM), X-ray photoelectron spectroscopy (XPS), atomic absorption spectroscopy and CO pulse chemisorption.

The monometallic Pt/TiO_2 catalyst prepared by flame spray pyrolysis was substituted by (F)-Pt/TiO_2 symbol. The bimetallic $Pt\text{-}Co/TiO_2$ catalyst was synthesized by flame spray pyrolysis and substituted by (F) $Pt\text{-}Co/TiO_2$ symbol. The synthesized nanoparticles were denoted as (F or I) - XCo/TiO_2 where X is Co loading contents in wt%.

4.2.1 X-ray diffraction (XRD)

The XRD patterns of monometallic Pt/TiO_2 and bimetallic $Pt\text{-}Co/TiO_2$ catalysts synthesized by flame spray pyrolysis method are shown in Figure 4.9. Both monometallic and bimetallic catalysts exhibited the characteristic peaks of anatase TiO_2 at 2θ = 25° (major), 37°, 48°, 55°, 56°, 62°, 71°, and 75° and rutile phase at 2θ = 28° (major), 36°, 42°, and 57°[43]. The characteristic peaks corresponding to both anatase and rutile phases TiO_2 were observed on all samples. No sharp peaks for platinum and cobalt species observed in all the XRD patterns due to low amount of metals present and/or high dispersion of these metals on the TiO_2 supports. The

average crystallite sizes of anatase phase TiO_2 support were calculated by the Scherre's equation from the full width at half maximum of the XRD peak at 2θ=25°. The average crystallite size of anatase phase TiO_2 supports ananatase phase of the TiO_2 support of both synthesis catalysts are summarized in Table 4.3

Addition of Co resulted in a decrease of %anatase content from 89.6 to 57.0% as Co loading contents increased from 0 to 0.8 wt% and indicated little influence for average crystallite size of anatase phase TiO_2, which was approximate 11-12 nm. Decreasing of %anatase due to the addition of Co can cause TiO_2 structure modification. Cobalt generates oxygen deficiency and Co^{2+} substitution can concomitantly occur in the anatase lattice. Therefore, accumulated oxygen vacancies in anatase phase enable the phase transition to rutile. This result was similar to Giraldi, T. R. et al.[55]that synthesized Co/TiO_2 by using polymeric precursor method which was quite similar to flame spray pyrolysis.

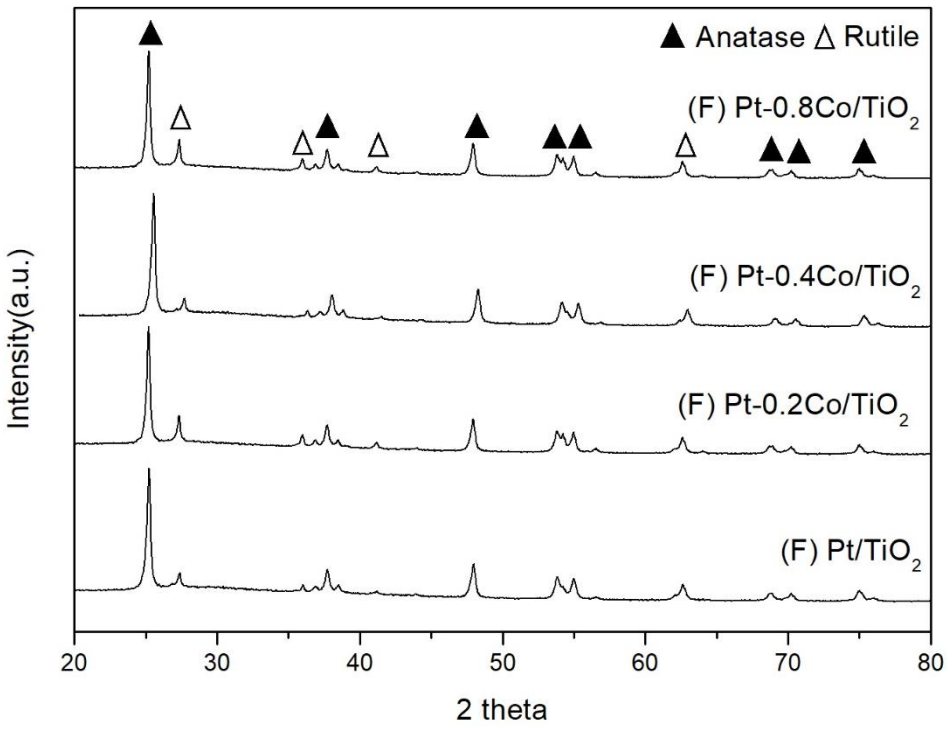

Figure 4.8 The XRD patterns of (F) Pt/TiO_2 and (F) $Pt\text{-}Co/TiO_2$ catalysts

4.2.2 N_2-physisorption

The BET surface area, pore volume, pore diameter and N_2 adsorption-desorption isotherms are determined by N_2-physisorption. The BET surface area, pore volume, and average pore diameter of the Pt/TiO_2 and Pt-Co/TiO_2 catalysts prepared by flame spray pyrolysis method are shown in Table 4.3 and The N_2 adsorption-desorption isotherms of the Pt/TiO_2 and Pt-Co/TiO_2 catalysts prepared by flame spray pyrolysis method are shown in Figure 4.10.

The (F) Pt/TiO_2 catalyst showed BET surface area, pore volume, and pore diameter at 42.6 m^2/g, 14 nm and 0.12 cm^3 (STP)/g, respectively. For bimetallic catalysts, Co adding into Pt/TiO_2 catalyst led to higher BET surface area. The metal doping could prevent the growth of the TiO_2 particles. Pongthawornsakun, B. et al. [43] also reported higher BET surface area of Pd/TiO_2 and Ag/TiO_2 catalyst prepared by flame spray pyrolysis than TiO_2 prepared by flame spray pyrolysis. From the observation, it was found that when more Co was added BET surface area and pore volume obviously increased. From the N_2 adsorption-desorption isotherms results, both Pt/TiO_2 and Pt-Co/TiO_2 catalysts prepared by flame spray pyrolysis exhibited type IV physisorption isotherm with hysteresis loop, corresponding the characteristic of mesoporous materials with pore diameters between 2 and 50 nm and showed the hysteresis loop of type H3 indicating the slit shaped pores and/or panel-shaped particles.

Table 4.4 Physical properties of (F) Pt/TiO_2 and (F) $Pt\text{-}Co/TiO_2$catalysts

Catalyst	Crystallite size of anatase TiO_2[a] (nm)	%Phase composition[a]		BET surface areas (m^2/g)	Average pore diameter[b] (nm)	Pore volume[b] (cm^3(STP)/g)
		Anatase	Rutile			
(F) Pt/TiO_2	12.4	89.6	10.4	42.6	14.0	0.12
(F) $Pt\text{-}0.2Co/TiO_2$	12.4	82.4	17.6	44.5	10.7	0.11
(F) $Pt\text{-}0.4Co/TiO_2$	11.6	69.0	31.0	49.8	10.6	0.10
(I) $Pt\text{-}0.8Co/TiO_2$	11.9	57.0	43.0	72.3	10.8	0.27

[a] Base on the XRD results

[b] Determined from the Barret-Joyner-Halenda(BJH) desorption method

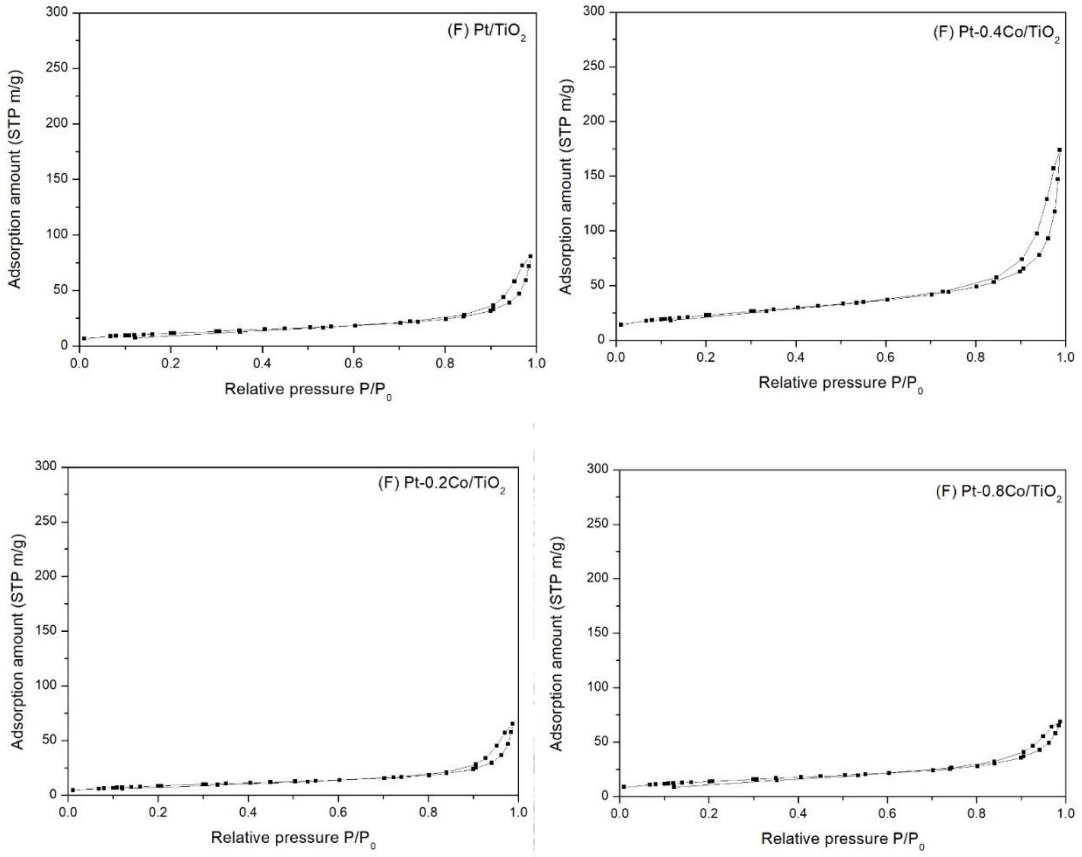

Figure 4.9 The N_2 adsorption-desorption isotherms of (F) Pt/TiO_2 and (F) $Pt\text{-}Co/TiO_2$ catalysts

4.2.3 H_2-temperature programmed reduction (H_2-TPR)

The H_2-TPR measurements were carried out to study the reduction behaviors of the monometallic Pt/TiO_2 and bimetallic $Pt\text{-}Co/TiO_2$ catalysts prepared by flame spray pyrolysis. The results are shown in Figure 4.11. Both of monometallic Pt/TiO_2 and bimetallic $Pt\text{-}Co/TiO_2$ catalysts showed three reduction peaks at 94-100 °C, 321-331 °C and 509-545 °C. The first reduction peak was correlated to the reduction of PtO_x to metallic Pt^0 [23, 47]. The second reduction peak was associated to reduction of Pt species interacting with the TiO_2 support to form $Pt\text{-}TiO_x$ interface site[23, 48] and third reduction peak is the hydrogen consumption above 500 °C due to the reduction of surface capping oxygen of TiO_2 [23].

For the bimetallic catalysts, the first reduction peaks were shifted to higher reduction temperatures when Co content was increased to 0.4-0.8 wt%. Addition of second metals can result in a decoration effect in which the reduction temperature increase [48]. The second reduction peaks were shifted to higher reduction temperatures when Co was added to the Pt/TiO_2 catalysts, suggesting stronger interaction between metal and TiO_2 support. It is also possible that some cobalt particles migrated onto the Pt surface[7].

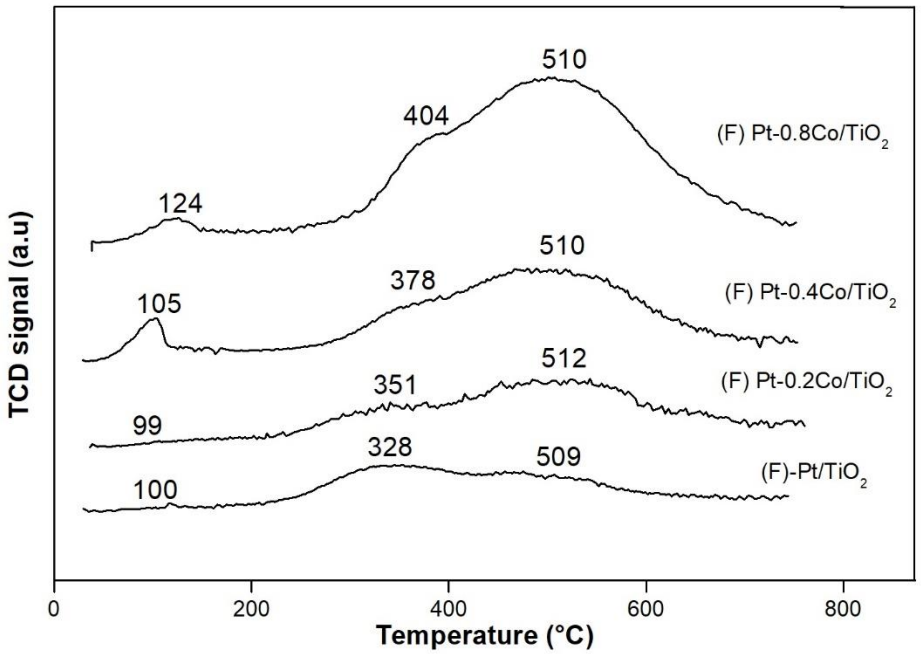

Figure 4.10 H_2-TPR profiles of (F) Pt/TiO_2 and (F) $Pt\text{-}Co/TiO_2$ catalysts

4.1.4 Transmission electron spectroscopy (TEM)

The morphology and metal particles size of catalysts can be found from TEM analysis. The TEM images of (F) Pt/TiO_2 and (F) $Pt\text{-}0.8Co/TiO_2$ catalysts are shown in Figure 4.12-4.13, respectively.

The (F) Pt/TiO_2 catalyst showed metal particles size at 5.4 nm. Addition of Co resulted in a decrease of metal particles size from 5.4 nm to very small that they cannot be observed in the TEM images as shown for Co loading contents from 0 to 0.8 wt%. In addition, The (F) Pt-0.8Co/TiO_2 catalyst presented smaller Pt particles size and a stronger interaction between metal and TiO_2 support catalyst than (F) Pt/TiO_2 catalyst therefore it was difficult to have surface migration of metal particles. As a consequence, metal particles size decreased [49], corresponding to the H_2-TPR results.

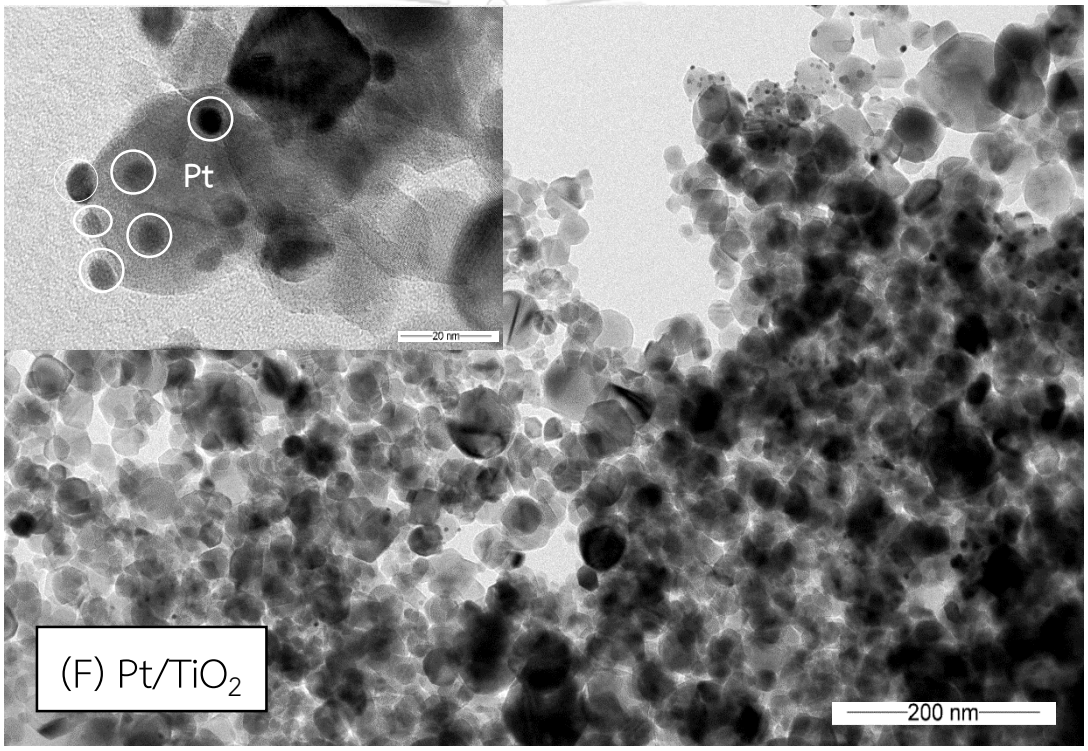

Figure 4.11 TEM images of the (F) Pt/TiO_2 catalyst

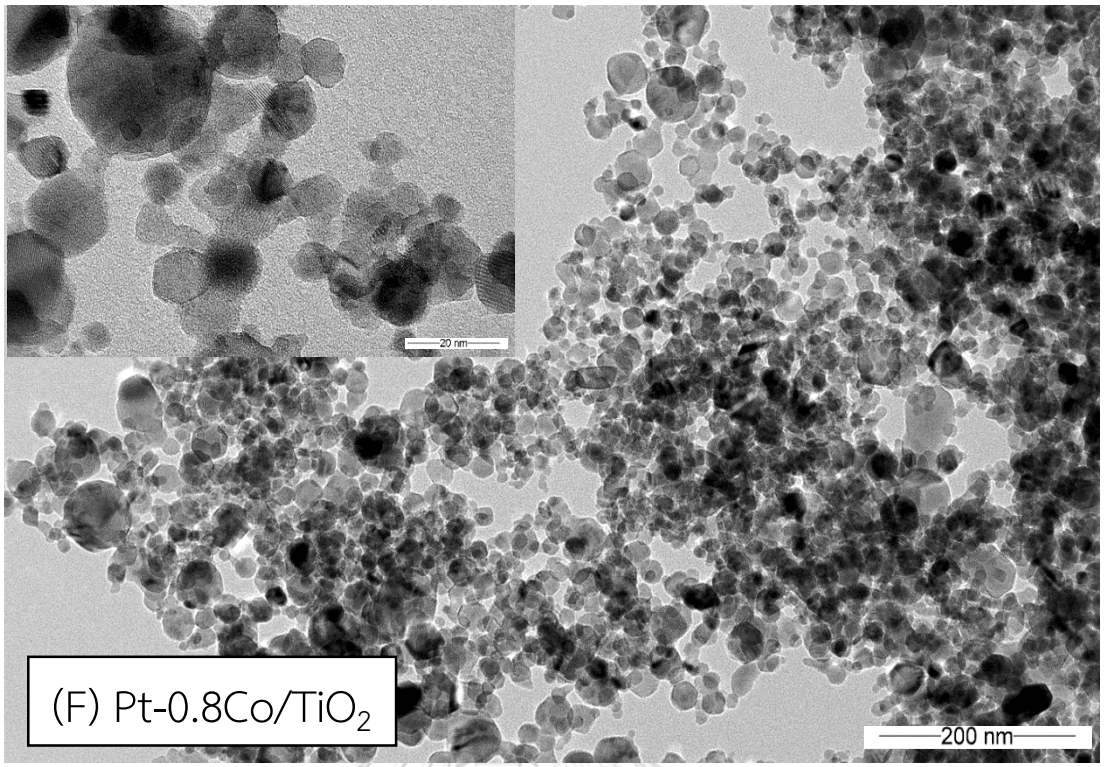

Figure 4.12 TEM images of the (F) Pt-0.8Co/TiO_2 catalyst

4.2.5 X-ray photoelectron spectroscopy (XPS)

The elemental composition of the catalyst at surface and electronic states were investigated by X-ray photoelectron spectroscopy (XPS). The XPS spectra of Ti 2p, the XPS spectra of Ti 2p of (F) Pt/TiO_2 and (F) Pt-0.8Co/TiO_2 catalysts are shown in Figure 4.14. There are two peaks at around 458.9 eV and 464.6 eV which corresponded to the $Ti2p_{3/2}$ and $Ti2p_{1/2}$, respectively[50]. These values were corresponding to the Ti^{4+}.

For bimetallic Pt-Co/TiO_2 catalysts, the peak of $Ti2p_{3/2}$ and $Ti2p_{1/2}$ was shifted to lower binding energies when comparing with flame made Pt/TiO_2 catalyst. It is suggested that there was a stronger interaction between metal and support TiO_2 for the bimetallic catalysts [56].

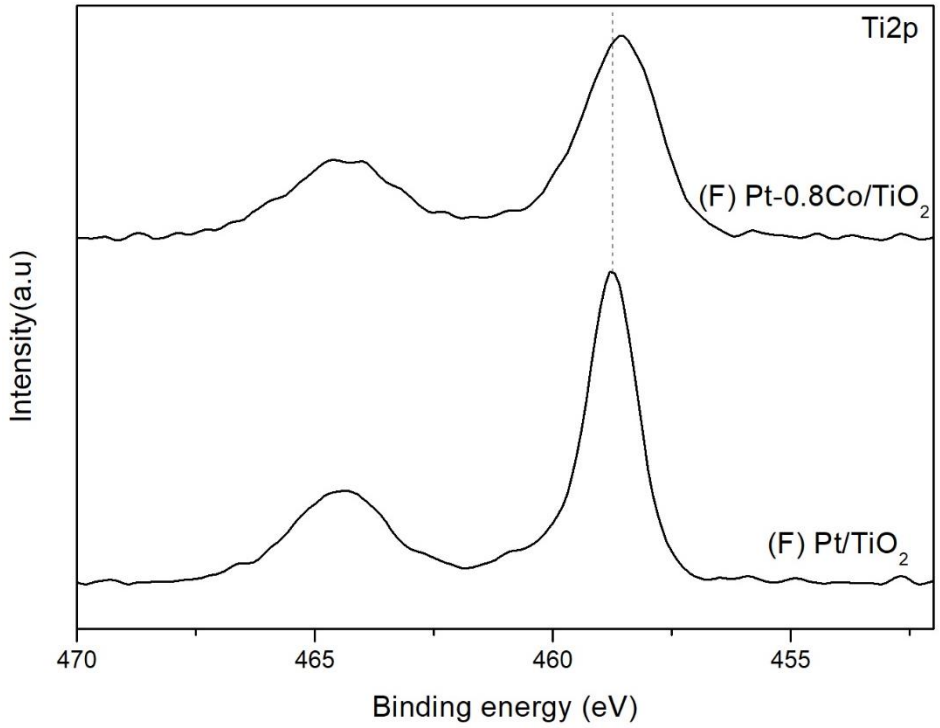

Figure 4.13 The XPS spectra of Ti 2p, the XPS spectra of Ti 2p of (F) Pt/TiO_2 and (F) $Pt\text{-}0.8Co/TiO_2$ catalysts

4.2.6 CO pulse chemisorption

The amounts of active Pt sites and %Pt dispersion on the catalyst samples were estimated from CO chemisorption. Both of the Pt/TiO_2 and $Pt\text{-}Co/TiO_2$ catalysts were reduced under H_2 flow at 500 °C before CO injection to adsorb on active sites. The %Pt dispersion were determined based on the assumption that one molecule of CO adsorbed on one molecule of Pt and none of CO molecule adsorbed on Co sites as our research group tested Co/TiO_2 catalyst by CO chemisorption, they found that very little CO adsorbed on Co/TiO_2. The % Pt dispersion and amount of active sites of Pt/TiO_2 and Pt/Co-modified TiO_2 of impregnated catalysts are shown in Table 4.4.

The monometallic flame made Pt/TiO_2 catalyst exhibited the amount of active Pt sites and %Pt dispersion at 3.1 $x10^{18}$moleculsCO/g and 19.2%, respectively. And when Co was added into Pt/TiO_2 catalyst, amounts of active Pt sites and %Pt dispersion increased which may be because Co addition can enhance CO adsorption on catalyst by modification of surface of platinum, forming a sandwich structure[51].

Table 4.5 CO chemisorption results of (F) Pt/TiO_2 and (F) $Pt\text{-}Co/TiO_2$ catalysts

Catalyst	Pt actual loading[a] (wt%)	Co actual loading[a] (wt%)	Amount of active sites ($x10^{18}$) ($x10^{18}$molecule CO/g cat)	% Pt dispersion[b]
(F) Pt/TiO_2	0.66	-	3.1	19.2
(F) $Pt\text{-}0.2Co/TiO_2$	0.65	0.20	3.1	20.1
(F) $Pt\text{-}0.4Co/TiO_2$	0.74	0.48	7.8	42.4
(F) $Pt\text{-}0.8Co/TiO_2$	0.67	0.80	9.5	52.5

[a] Results from Atomic absorption spectroscopy

[b] Calculations based on Pt actual loading from atomic absorption spectroscopy

4.2.7 Evaluation of the catalyst performance in the selective furfural hydrogenation

The catalytic behaviors of the monometallic Pt/TiO_2 and bimetallic Pt-Co/TiO_2 catalysts prepared by flame spray pyrolysis including furfural conversion and product selectivity are summarized in Table 4.4

The monometallic (F) Pt/TiO_2 catalyst showed furfural conversion and FA selectivity at 83.4% and 95.1%, respectively. For bimetallic, Co addition into monometallic Pt/TiO_2 catalyst affect to increased FA selectivity but decreased furfural conversion. According to the XPS results, addition of Co into flame made Pt/TiO_2 catalyst affected to peak of $Ti2p_{3/2}$ and $Ti2p_{1/2}$ by shifting to lower binding energy, which suggested the Ti^{x+} (X<4) formation. From H_2-TPR results, the second reduction peaks were also shifted to higher temperature reduction suggesting a stronger metal and TiO_2 support interaction. From these reasons, FA selectivity was enhanced due to creation of metal–TiO_2 sites from TiO_x which Pt particles migrated to and decorated on TiO_2 support, which facilitating the hydrogenation of C=O bond[52]. From CO-chemisorption results, the %Pt dispersion was increased when Co adding into flame made Pt/TiO_2 catalyst. It may be suggested that %Pt dispersion was correlated with the presence of surface Ti^{3+}[57, 58] leading to improved FA selectivity, corresponding to both XPS and H_2-TPR results. Decreasing of furfural conversion related to decreasing of %anatase phase when Co adding into flame made Pt/TiO_2 catalyst because metal on rutile phase from TiO_2 support was weakly interacted with hydrogen molecules [54].

Table 4.6 The reaction results of (F) Pt/TiO_2 and (F) $Pt-Co/TiO_2$ catalysts

Catalyst	%Conversion	%Selectivity		%Yield of FA
		FA	SP	
(F) Pt/TiO_2	83.4	95.1	4.9	79.3
(F) $Pt-0.2Co/TiO_2$	71.1	95.5	4.5	67.9
(F) $Pt-0.4Co/TiO_2$	68.3	97.2	2.8	66.4
(F) $Pt-0.8Co/TiO_2$	47.3	100	0	47.3

Reaction (50 µL furfural in 10 ml methanol) at 50 °c with a 50 mg catalyst under 20 bar H_2 after 120 min

FA = Furfuryl alcohol

SP = Solvent product

4.2.8 Comparison between flame spray pyrolysis and impregnation method of both of monometallic Pt/TiO_2 catalysts and bimetallic Pt-Co/TiO_2 catalysts.

The catalytic performance of (F) Pt/TiO_2, (I) Pt/TiO_2, (F) Pt-0.2Co/TiO_2 and (I) Pt-0.2Co/TiO_2, (F) Pt-0.4Co/TiO_2 and (I) Pt-0.4Co/TiO_2 catalysts in the selective furfural hydrogenation are shown in Table.4.5.

For the monometallic Pt/TiO_2 catalysts, the (F) Pt/TiO_2 catalyst showed similar furfural conversion and higher FA selectivity than (I) Pt/TiO_2 catalyst. From the XPS and H_2-TPR results, the XPS spectra peaks of $Ti2p_{3/2}$ and $Ti2p_{1/2}$ of (F) Pt/TiO_2 catalyst shifted to lower binding which suggested to Ti^{x+} ($x < 4$) formation and the second reduction peak of (F) Pt/TiO_2 was also shifted to higher temperature due to stronger interaction between Pt and TiO_2 support to form Pt-TiO_x interface sites, consequencely the FA selectivity increased. The (F) Pt/TiO_2 catalyst showed higher FA yield than (I) Pt/TiO_2 catalyst.

For the bimetallic Pt-0.2Co/TiO_2 catalysts, the impregnated Pt-0.2Co/TiO_2 catalyst showed higher furfural conversion and similar FA selectivity to flame made Pt-0.2Co/TiO_2 catalyst. Because the impregnated Pt-0.2Co/TiO_2 catalyst indicated higher %anatase phase of TiO_2 support than flame made Pt-0.2Co/TiO_2 catalyst, hydrogen molecules adsorbed on impregnated Pt-0.2Co/TiO_2 catalyst better than flame made Pt-0.2Co/TiO_2 catalysts, the hydrogenation activity was therefore higher on the impregnated Pt-0.2Co/TiO_2 catalysts. For bimetallic Pt-0.4Co/TiO_2 catalyst, the (I) Pt-0.4Co/TiO_2 catalyst showed both lower both furfural conversion and FA selectivity because of low amount of Pt-TiOx species, Co-PtTiOx species and Pt/Ti ratio. Among the catalysts synthesized in this work, the bimetallic Pt-0.2Co/TiO_2 catalyst prepared by impregnation method was the most efficient catalyst for selective hydrogenation of furfural to furfuryl alcohol due to the highest FA yield.

Compared to the literature reported about the hydrogenation of furfural to furfuryl alcohol (Table 4.8), the catalysts synthesized in this work showed high furfural conversion and furfuryl alcohol selectivity under mild conditions (50℃, 2MPa) and shorter reaction time (2h).

Table 4.7 the reaction results of (F) Pt/TiO_2, (I) Pt/TiO_2, (F) Pt-0.2Co/TiO_2, (I) Pt-0.2Co/TiO_2, (F) Pt-0.4Co/TiO_2 and (I) Pt-0.4Co/TiO_2 catalysts

Catalyst	%Conversion	%Selectivity		%Yield of FA
		FA	SP	
(F) Pt/TiO_2	83.4	95.1	4.9	79.3
(I) Pt/TiO_2	84.6	71.5	28.5	60.5
(F) Pt-0.2Co/TiO_2	71.1	95.5	4.5	67.9
(I) Pt-0.2Co/TiO_2	100	97.5	2.5	97.5
(F) Pt-0.4Co/TiO_2	68.3	97.2	2.8	66.4
(I) Pt-0.4Co/TiO_2	45.1	49.8	50.2	22.5

Reaction (50 µL furfural in 10 ml methanol) at 50 °c with a 50 mg catalyst under 20 bar H_2 after 120 min

FA = Furfuryl alcohol

SP = Solvent product

Table 4.8 Comparison between synthesized catalyst and other catalysts reported in the literature

No.	Catalysts	Reaction conditions	Reaction time	Result	Ref.
1	(I) Pt-0.2Co/TiO_2	50 °C, 2 MPa of H_2	2 hr	Furfural conversion = 100% FA selectivity= 97.5%	This work
2	Pt-Re/TiO_2-ZrO_2	130 °C, 5 MPa of H_2	8 hr	Furfural conversion = 100% FA selectivity= 2.1%	[5]
3	Pt/ɣ-Al_2O_3	50 °C, ambient of H_2	7 hr	Furfural conversion = 80% FA selectivity= 99%	[2]
4	Pt/MgO	50 °C, ambient of H_2	7 hr	Furfural conversion = 79% FA selectivity= 97%	[2]
5	Pt/CeO_2	50 °C, ambient of H_2	7 hr	Furfural conversion = 77% FA selectivity= 98%	[2]
6	Ni-Pt/SiO_2	250 °C, 0.68 MPa of H_2	1.5 hr	Furfural conversion = 43.3% FA selectivity= 38.5%	[4]
7	Cu-Pt/SiO_2	250 °C, 0.68 MPa of H_2	1.5 hr	Furfural conversion = 15.3% FA selectivity= 90.5%	[4]
8	Pt/SiO_2	250 °C, 0.68 MPa of H_2	1.5 hr	Furfural conversion = 12.5% FA selectivity= 55.8%	[4]
9	Pt/SiO_2	100 °C, 1 MPa of H_2	8 hr	Reaction rate = 0.38 mmol/gPt s FA selectivity= 98.7%	[3]
10	Pt-Sn/SiO_2	100 °C, 1 MPa of H_2	8 hr	Reaction rate = 2.3 mmol/gPt s FA selectivity= 96.2%	[3]
11	Pt/Al_2O_3	25 °C, 6 MPa of H_2	1 hr	Furfural conversion = 65.6% FA selectivity= 99.7%	[1]
12	Pt/Al_2O_3	25 °C, 6 MPa of H_2	1 hr	Furfural conversion = 80.3% FA selectivity= 2.6%	[1]
13	Pd/SiO_2	250 °C, 4 MPa of H_2	1 hr	Furfural conversion = 68% FA selectivity= 10.3%	[59]

No.	Catalysts	Reaction conditions	Reaction time	Result	Ref.
14	Pd-Fe/SiO_2	250 °C, 4 MPa of H_2	1 hr	Furfural conversion = 84% FA selectivity= 25%	[59]
15	Pd-Fe/ ɣ-Al_2O_3	250 °C, 4 MPa of H_2	1 hr	Furfural conversion = 89% FA selectivity= 7.9%	[59]
16	CuCo/C	140 °C, 3 MPa of H_2	1 hr	Furfural conversion = 99% FA selectivity= 97.3%	[42]
17	Ru/C	90 °C, 1.25 MPa of H_2	5 hr	Furfural conversion = 85% FA selectivity= 47%	[39]
18	Ru-Sn/C	90 °C, 1.25 MPa of H_2	5 hr	Furfural conversion = 95% FA selectivity= 90%	[39]
19	Ir/TiO_2	90 °C, 0.62 MPa of H_2	2 hr	Furfural conversion = 30% FA selectivity= 100%	[60]
20	Cu/SiO_2	100 °C, 2 MPa of H_2	5 hr	Furfural conversion = 29% FA selectivity < 1%	[41]
21	Pt/SiO_2	100 °C, 2 MPa of H_2	5 hr	Furfural conversion = 31% FA selectivity = 29 %	[41]
22	Pd/SiO_2	100 °C, 2 MPa of H_2	5 hr	Furfural conversion = 44% FA selectivity = 10 %	[41]
23	Ni/CNT	130 °C, 4 MPa of H_2	10 hr	Furfural conversion = 99.1% FA selectivity = 2.1 %	[61]
24	Ni-Cu/CNT	130 °C, 4 MPa of H_2	10 hr	Furfural conversion = 100% FA selectivity = 0.2 %	[61]
25	Ni/TiO_2	130 °C, 4 MPa of H_2	10 hr	Furfural conversion = 13% FA selectivity = 69.5 %	[61]
26	Ni/ ɣ-Al_2O_3	130 °C, 4 MPa of H_2	10 hr	Furfural conversion = 31.4% FA selectivity = 70.4 %	[61]

CHARPTER V
CONCLUSIONS AND RECOMMENDATIONS

5.1 Conclusions

Co loading on the monometallic Pt/TiO_2 catalyst by impregnation method prevented anatase to rutile TiO_2 phase transformation, increased %Pt dispersion and exhibited a stronger interaction between metal and TiO_2 support. The catalytic performances of the bimetallic catalysts (impregnation) in selective furfural hydrogenation were improved in terms of both furfural conversion and FA selectivity. Additionally, optimal Co loading was determined to be at 0.2wt%.

On the other hand, Co loading on Pt/TiO_2 catalyst synthesized by flame spray pyrolysis accelerated anatase to rutile transformation but increased %Pt dispersion and exhibited stronger interaction between metal and TiO_2 support. As a consequence, the furfural conversion decreased but FA selectivity increased for the flame-made bimetallic catalysts.

Considering the effect of preparation method, despite its lower %Pt dispersion, the flame made monometallic Pt/TiO_2 catalyst exhibited similar furfural conversion but higher FA selectivity than impregnated monometallic Pt/TiO_2 catalyst. These could be attributed to similar %anatase phase of TiO_2 support for both catalysts but the flame made monometallic Pt/TiO_2 catalyst exhibited a stronger interaction between Pt and TiO_2 support. For the bimetallic $PtCo/TiO_2$ synthesized catalysts, it was found that the (I) $Pt\text{-}0.2Co/TiO_2$ catalysts showed the best catalytic performance for selective hydrogenation of furfural to furfuryl alcohol because the impregnated $Pt\text{-}0.2Co/TiO_2$ catalyst had both high %anatase phase of TiO_2 support and strong interaction between metal and TiO_2 support.

5.2 Recommendations

1. Characteristic of bimetallic PtCo nanoparticles supported on TiO_2 should be investigated by high resolution analytical equipment such as high resolution TEM.

2. Type of Pt species on catalyst should be further characterized by CO-IR.

3. The reusability and/or regeneration of the synthesized catalysts should be investigated in the selective hydrogenation of furfural.

REFERENCES

[1] S. Bhogeswararao and D. Srinivas, "Catalytic conversion of furfural to industrial chemicals over supported Pt and Pd catalysts," *Journal of Catalysis,* vol. 327, pp. 65-77, 2015.

[2] M. J. Taylor *et al.*, "Highly selective hydrogenation of furfural over supported Pt nanoparticles under mild conditions," *Applied Catalysis B: Environmental,* vol. 180, pp. 580-585, 2016.

[3] A. B. Merlo, V. Vetere, J. F. Ruggera, and M. L. Casella, "Bimetallic PtSn catalyst for the selective hydrogenation of furfural to furfuryl alcohol in liquid-phase," *Catalysis Communications,* vol. 10, no. 13, pp. 1665-1669, 2009.

[4] C. Zhang, Q. Lai, and J. H. Holles, "Bimetallic overlayer catalysts with high selectivity and reactivity for furfural hydrogenation," *Catalysis Communications,* vol. 89, pp. 77-80, 2017.

[5] B. Chen, F. Li, Z. Huang, and G. Yuan, "Tuning catalytic selectivity of liquid-phase hydrogenation of furfural via synergistic effects of supported bimetallic catalysts," *Applied Catalysis A: General,* vol. 500, pp. 23-29, 2015.

[6] R. Zheng, M. D. Porosoff, J. L. Weiner, S. Lu, Y. Zhu, and J. G. Chen, "Controlling hydrogenation of CO and CC bonds in cinnamaldehyde using silica supported Co-Pt and Cu-Pt bimetallic catalysts," *Applied Catalysis A: General,* vol. 419-420, pp. 126-132, 2012.

[7] S. Pisduangdaw, O. Mekasuwandumrong, S.-I. Fujita, M. Arai, H. Yoshida, and J. Panpranot, "One step synthesis of Pt–Co/TiO2 catalysts by flame spray pyrolysis for the hydrogenation of 3-nitrostyrene," *Catalysis Communications,* vol. 61, pp. 11-15, 2015.

[8] G. Solero, "Synthesis of Nanoparticles through Flame Spray Pyrolysis: Experimental Apparatus and Preliminary Results," *Nanoscience and Nanotechnology* vol. 7, pp. 21-25, 2017.

[9] M. Høj, K. Linde, T. K. Hansen, M. Brorson, A. D. Jensen, and J.-D. Grunwaldt, "Flame spray synthesis of CoMo/Al_2O_3 hydrotreating catalysts," *Applied Catalysis A: General,* vol. 397, no. 1-2, pp. 201-208, 2011.

[10] S. Somboonthanakij *et al.*, "Characteristics and Catalytic Properties of Pd/SiO_2 Synthesized by One-step Flame Spray Pyrolysis in Liquid-phase Hydrogenation of 1-Heptyne," *Catalysis Letters,* vol. 119, no. 3-4, pp. 346-352, 2007.

[11] S. Pisduangdaw *et al.*, "Characteristics and catalytic properties of Pt–Sn/Al_2O_3 nanoparticles synthesized by one-step flame spray pyrolysis in the dehydrogenation of propane," *Applied Catalysis A: General,* vol. 370, no. 1-2, pp. 1-6, 2009.

[12] F. Nerozzi, "Heterogeneous Catalytic Hydrogenation," *Platinum Metals Review,* vol. 56, no. 4, pp. 236-241, 2012.

[13] R. D. M. a. J. K. Erica Farnetti, "HOMOGENEOUS AND HETEROGENEOUS CATALYSIS," *INORGANIC AND BIO-INORGANIC CHEMISTRY,* vol. 2.

[14] P. N. Rylander, "PLATINUM METALS IN CATALYTIC HYDROGENATION."

[15] P. A. f. https://en.wikipedia.org/wiki/Platinum.

[16] R. M. D. Nunes, B. F. Machado, M. M. Pereira, M. J. S. M. Moreno, and J. L. Faria, "Platinum supported on TiO_2 as a new selective catalyst on heterogeneous hydrogenation of α,β-unsaturated oxosteroids," *Journal of Molecular Catalysis A: Chemical,* vol. 333, no. 1-2, pp. 1-5, 2010.

[17] S. Bagheri, N. Muhd Julkapli, and S. Bee Abd Hamid, "Titanium dioxide as a catalyst support in heterogeneous catalysis," *ScientificWorldJournal,* vol. 2014, p. 727496, 2014.

[18] T. Ohno, K. Sarukawa, K. Tokieda, and M. Matsumura, "Morphology of a TiO_2 Photocatalyst (Degussa, P-25) Consisting of Anatase and Rutile Crystalline Phases," *Journal of Catalysis,* vol. 203, no. 1, pp. 82-86, 2001.

[19] v. N. S.A. Ananthan, "TiO_2 Supported Ru and Pt Nano Catalysts for Selective Hydrogenation of Citral," 2011.

[20] S. S. Peter Claus, Rainer Sch6del, Peter Kraak, Wolfgang M6rke, Dieter H6nicke, "Hydrogenation of crotonaldehyde on Pt/TiO_2 catalysts: Influence of the phase

composition of titania on activity and intramolecular selectivity," *Applied Catalysis A,* vol. 165, pp. 429-441, 1997.

[21] A. J. Martin Englisch, and Johannes A. Lercher, "Structure Sensitivity of the Hydrogenation of Crotonaldehyde over Pt/SiO_2 and Pt/TiO_2," *JOURNAL OF CATALYSIS* vol. 166, pp. 25-35, 1997.

[22] R. Mueller, L. Mädler, and S. E. Pratsinis, "Nanoparticle synthesis at high production rates by flame spray pyrolysis," *Chemical Engineering Science,* vol. 58, no. 10, pp. 1969-1976, 2003.

[23] S. Pisduangdaw, O. Mekasuwandumrong, H. Yoshida, S.-I. Fujita, M. Arai, and J. Panpranot, "Flame-made Pt/TiO_2 catalysts for the liquid-phase selective hydrogenation of 3-nitrostyrene," *Applied Catalysis A: General,* vol. 490, pp. 193-200, 2015.

[24] G. Liu *et al.*, "Catalytic oxidation of benzene over Ce–Mn oxides synthesized by flame spray pyrolysis," *Particuology,* vol. 11, no. 4, pp. 454-459, 2013.

[25] O. Mekasuwandumrong, S. Phothakwanpracha, B. Jongsomjit, A. Shotipruk, and J. Panpranot, "Liquid-Phase Selective Hydrogenation of 1-Heptyne over Pd/TiO_2 Catalyst Synthesized by One-Step Flame Spray Pyrolysis," *Catalysis Letters,* vol. 136, no. 1-2, pp. 164-170, 2010.

[26] B. Schimmoeller, R. Delaigle, D. P. Debecker, and E. M. Gaigneaux, "Flame-made vs. wet-impregnated vanadia/titania in the total oxidation of chlorobenzene: Possible role of VOx species," *Catalysis Today,* vol. 157, no. 1-4, pp. 198-203, 2010.

[27] J. Huang, Y. Jiang, N. van Vegten, M. Hunger, and A. Baiker, "Tuning the support acidity of flame-made Pd/SiO_2–Al_2O_3 catalysts for chemoselective hydrogenation," *Journal of Catalysis,* vol. 281, no. 2, pp. 352-360, 2011.

[28] R. Strobel, J.-D. Grunwaldt, A. Camenzind, S. E. Pratsinis, and A. Baiker, "Flame-made Alumina Supported Pd–Pt Nanoparticles: Structural Properties and Catalytic Behavior in Methane Combustion," *Catalysis Letters,* vol. 104, no. 1-2, pp. 9-16, 2005.

[29] C.-Y. Chiang, K. Aroh, N. Franson, V. R. Satsangi, S. Dass, and S. Ehrman, "Copper oxide nanoparticle made by flame spray pyrolysis for

photoelectrochemical water splitting – Part II. Photoelectrochemical study," *International Journal of Hydrogen Energy,* vol. 36, no. 24, pp. 15519-15526, 2011.

[30] G. L. Chiarello, E. Selli, and L. Forni, "Photocatalytic hydrogen production over flame spray pyrolysis-synthesised TiO_2 and Au/TiO_2," *Applied Catalysis B: Environmental,* vol. 84, no. 1-2, pp. 332-339, 2008.

[31] M. Minnermann *et al.*, "Double flame spray pyrolysis as a novel technique to synthesize alumina-supported cobalt Fischer–Tropsch catalysts," *Catalysis Today,* vol. 214, pp. 90-99, 2013.

[32] M. J. Height, S. E. Pratsinis, O. Mekasuwandumrong, and P. Praserthdam, "Ag-ZnO catalysts for UV-photodegradation of methylene blue," *Applied Catalysis B: Environmental,* vol. 63, no. 3-4, pp. 305-312, 2006.

[33] R. Strobel, "Flame-made platinum/alumina: structural properties and catalytic behaviour in enantioselective hydrogenation," *Journal of Catalysis,* vol. 213, no. 2, pp. 296-304, 2003.

[34] E. C. Lovell, J. Scott, and R. Amal, "Ni-SiO_2 catalysts for the carbon dioxide reforming of methane: varying support properties by flame spray pyrolysis," *Molecules,* vol. 20, no. 3, pp. 4594-609, Mar 12 2015.

[35] "https://en.wikipedia.org/wiki/Cobalt#Applications."

[36] "https://www.lenntech.com/periodic/elements/co.htm."

[37] N. M. Bertero, A. F. Trasarti, B. Moraweck, A. Borgna, and A. J. Marchi, "Selective liquid-phase hydrogenation of citral over supported bimetallic Pt–Co catalysts," *Applied Catalysis A: General,* vol. 358, no. 1, pp. 32-41, 2009.

[38] B. G. A. Armando Borgna, Abdool M. Saib,Hendrik Bluhm,, A. K.-G. Michael Ha1vecker, A. E. T. (Ton) Kuiper,Yde Tamminga, and, and J. W. H. Niemantsverdriet, "Pt-Co/SiO_2 Bimetallic Planar Model Catalysts for Selective Hydrogenation of Crotonaldehyde," *J. Phys. Chem.,* vol. 108, pp. 17905-17914, 2004.

[39] J. J. Musci, A. B. Merlo, and M. L. Casella, "Aqueous phase hydrogenation of furfural using carbon-supported Ru and RuSn catalysts," *Catalysis Today,* vol. 296, pp. 43-50, 2017.

[40] K. Fulajtárova, T. Soták, M. Hronec, I. Vávra, E. Dobročka, and M. Omastová, "Aqueous phase hydrogenation of furfural to furfuryl alcohol over Pd–Cu catalysts," *Applied Catalysis A: General,* vol. 502, pp. 78-85, 2015.

[41] Á. O'Driscoll, J. J. Leahy, and T. Curtin, "The influence of metal selection on catalyst activity for the liquid phase hydrogenation of furfural to furfuryl alcohol," *Catalysis Today,* vol. 279, pp. 194-201, 2017.

[42] Y. Wang, Y. Miao, S. Li, L. Gao, and G. Xiao, "Metal-organic frameworks derived bimetallic Cu-Co catalyst for efficient and selective hydrogenation of biomass-derived furfural to furfuryl alcohol," *Molecular Catalysis,* vol. 436, pp. 128-137, 2017.

[43] B. Pongthawornsakun, S.-i. Fujita, M. Arai, O. Mekasuwandumrong, and J. Panpranot, "Mono- and bi-metallic Au–Pd/TiO_2 catalysts synthesized by one-step flame spray pyrolysis for liquid-phase hydrogenation of 1-heptyne," *Applied Catalysis A: General,* vol. 467, pp. 132-141, 2013.

[44] G. B. Song, J. K. Liang, F. S. Liu, T. J. Peng, and G. H. Rao, "Preparation and phase transformation of anatase–rutile crystals in metal doped TiO_2/muscovite nanocomposites," *Thin Solid Films,* vol. 491, no. 1-2, pp. 110-116, 2005.

[45] O. Ola and M. M. Maroto-Valer, "Review of material design and reactor engineering on TiO_2 photocatalysis for CO2 reduction," *Journal of Photochemistry and Photobiology C: Photochemistry Reviews,* vol. 24, pp. 16-42, 2015.

[46] D. A. H. Hanaor and C. C. Sorrell, "Review of the anatase to rutile phase transformation," *Journal of Materials Science,* vol. 46, no. 4, pp. 855-874, 2010.

[47] C. Zhang, H. He, and K.-i. Tanaka, "Catalytic performance and mechanism of a Pt/TiO2 catalyst for the oxidation of formaldehyde at room temperature," *Applied Catalysis B: Environmental,* vol. 65, no. 1-2, pp. 37-43, 2006.

[48] J. V. G. a. R. P. T. HUIZINGA, "A Temperature programmed reduction study of Pt on Al_2O_3 and TiO_2," *Applied Catalysis.,* vol. 10, pp. 199-213, 1984.

[49] R. Nie, J. Wang, L. Wang, Y. Qin, P. Chen, and Z. Hou, "Platinum supported on reduced graphene oxide as a catalyst for hydrogenation of nitroarenes," *Carbon,* vol. 50, no. 2, pp. 586-596, 2012.

[50] Z. Fu, J. Zhang, X. Yang, and W. Cao, "Preparation of nano-crystal N-Zn/TiO_2 anode films and the effects of co-sensitization on the performance of dye-sensitized solar cells," *Chinese Science Bulletin,* vol. 56, no. 19, pp. 2001-2008, 2011.

[51] T. s. H. a. L. z. G. Genmin Lu', "Correlation between chemisorption and the mechanism of carbon monoxide hydrogenation over Pt-Co/NaY catalysts," *Applied Catalysis A: General, ,* vol. 98, pp. 61-73, 1992.

[52] A. D. a. M. A. Vannice, "Crotonaldehyde Hydrogenation on Pt/TiO_2 and Ni/TiO_2 SMSI Catalysts," *Catalysis* vol. 183, pp. 344-354, 1999.

[53] U. A. w. a. A. Selloni, "Hydrogen interaction with the anatase TiO_2(101) surface," *Phys. Chem. Chem. Phys.,* vol. 14, pp. 16595–16602, 2012.

[54] Mazharul M. Islam, †,‡ Monica Calatayud,§,|| and a. G. Pacchioni, "Hydrogen Adsorption and Diffusion on the Anatase TiO_2(101) Surface: A First-Principles Investigation," *J. Phys. Chem. C,* vol. 115, pp. 6809–6814, 2011.

[55] T. R. Giraldi, J. A. Dias, C. M. Baggio, S. C. Maestrelli, and J. A. Oliveira, "Anatase-to-rutile transition in co-doped TiO_2 pigments," *Journal of Sol-Gel Science and Technology,* vol. 83, no. 1, pp. 115-123, 2017.

[56] J. B. Zhong *et al.*, "Characterization and photocatalytic property of Pd/TiO_2 with the oxidation of gaseous benzene," *J Hazard Mater,* vol. 168, no. 2-3, pp. 1632-5, Sep 15 2009.

[57] S. Riyapan, Y. Boonyongmaneerat, O. Mekasuwandumrong, P. Praserthdam, and J. Panpranot, "Effect of surface Ti3+ on the sol–gel derived TiO_2 in the selective acetylene hydrogenation on Pd/TiO_2 catalysts," *Catalysis Today,* vol. 245, pp. 134-138, 2015.

[58] P. P. Kongkiat Suriye, * and Bunjerd Jongsomjit, "Impact of Ti3+ Present in Titania on Characteristics and Catalytic Properties of the Co/TiO_2 Catalyst," *Industrial& Engineering Chemistry Research,* vol. 44, pp. 6599-6604, 2005.

[59] N. Pino, S. Sitthisa, Q. Tan, T. Souza, D. López, and D. E. Resasco, "Structure, activity, and selectivity of bimetallic Pd-Fe/SiO_2 and Pd-Fe/ γ -Al_2O_3 catalysts for the conversion of furfural," *Journal of Catalysis,* vol. 350, pp. 30-40, 2017.

[60] D. S. Patricio Reyes*, Cristian Campos y Marcelo Oportus, "Selective hydrogenation of furfural on Ir/TiO_2 catalyst," *Quim. Nova,* vol. 33, pp. 777-780, 2010.

[61] L. Liu, H. Lou, and M. Chen, "Selective hydrogenation of furfural to tetrahydrofurfuryl alcohol over Ni/CNTs and bimetallic Cu Ni/CNTs catalysts," *International Journal of Hydrogen Energy,* vol. 41, no. 33, pp. 14721-14731, 2016.

APPENDIX

APPENDIX A

CALCULATION FOR CATALYST PREPARATION

For monometallic catalyst, the 0.5%Pt/TiO_2 catalyst prepared by flame spray pyrolysis method was shown.

Reagents: Platinum(II)acetyl-acetonate 99.99%

Titanium(IV) butoxide reagent grade, 97%

Xylene 99.8%

Concentration metal = 0.3 mole/lit

Calculation for Pt (mol) : $\frac{\mathbf{0.5\ gPt \times 1molPt}}{\mathbf{195.23Pt}}$ = 2.56 × 10^{-3} molPt

Calculation for Ti (mol) : $\frac{\mathbf{99.5\ gPt \times 1molTi}}{\mathbf{79.8Ti}}$ = 1.25 molTi

Pt+Ti = 1.2526 mol

Based on 500 ml total solution

Metal = $\frac{\mathbf{0.3\ mole}}{\mathbf{lit}}$ × 0.5 lit = 0.15 mole

Calculation for Pt (mol) :

$\frac{\mathbf{0.15\ mole \times 2.56 \times 10^{-3} molPt}}{\mathbf{1.2526\ mole}}$ = 3.066 × 10^{-4} molPt

Calculation for Ti (mol) :

$\frac{\mathbf{0.15mole \times 1.25\ molTi}}{\mathbf{1.2526\ mole}}$ = 0.1497 molTi

Calculation for Pt precursor :

$$3.066 \times 10^{-4} \text{ molPt} \times \frac{1 \text{ mol Pt(precursor)} \times 393.29 \text{ Pt(precursor)}}{1 \text{ molPt} \times 1 \text{ mol Pt(precursor)} \times 0.9999}$$

= 0.1206 g.

Calculation for Ti precursor :

$$0.1497 \text{ molTi} \times \frac{1 \text{ mol Ti(precursor)} \times 340.32 \text{ Ti(precursor)}}{1 \text{ molTi} \times 1 \text{ mol Ti(precursor)} \times 0.97} = 52.52 \text{ g.}$$

For bimetallic catalyst, the 0.5%Pt-0.2Co/TiO_2 catalysts prepared by flame spray pyrolysis method was shown.

Reagents: Platinum(II)acetyl-acetonate 99.99%

Titanium(IV) butoxide reagent grade, 97%

Cobalt naphthenate, 6 wt% in mineral spirits

Xylene 99.8%

Concentration metal = 0.3 mole/lit

Calculation for Pt (mol) : $\frac{0.5 \text{ gPt} \times 1 \text{molPt}}{195.23 \text{Pt}} = 2.56 \times 10^{-3}$ molPt

Calculation for Co (mol) : $\frac{0.2 \text{ gCo} \times 1 \text{molCo}}{58.93 \text{Co}} = 3.39 \times 10^{-3}$ molCo

Calculation for Ti (mol) : $\frac{99.46 \text{ gPt} \times 1 \text{molTi}}{79.8 \text{Ti}} = 1.25$ molTi

Pt+Co+Ti = 1.2532 mol

Based on 500 ml total solution

$$\text{Metal} = \frac{0.3 \text{ mole}}{\text{lit}} \times 0.5 \text{ lit} = 0.15 \text{ mole}$$

Calculation for Pt (mol) :

$$\frac{0.15\ \text{mole} \times 2.56 \times 10^{-3}\ \text{molPt}}{1.2532\ \text{mole}} = 3.06 \times 10^{-4}\ \text{molPt}$$

Calculation for Co (mol) :

$$\frac{0.15\ \text{mole} \times 3.39 \times 10^{-3}\ \text{molCo}}{1.2532\ \text{mole}} = 4.06 \times 10^{-4}\ \text{molCo}$$

Calculation for Ti (mol) :

$$\frac{0.15\ \text{mole} \times 1.25\ \text{molTi}}{1.2532\ \text{mole}} = 0.15\ \text{molTi}$$

Calculation for Pt precursor :

$$3.06 \times 10^{-4}\ \text{molPt} \times \frac{1\ \text{mol Pt(precursor)} \times 393.29\ \text{Pt(precursor)}}{1\ \text{molPt} \times 1\ \text{mol Pt(precursor)} \times 0.9999}$$

=0.120g.

Calculation for Co precursor :

$$4.06 \times 10^{-4}\ \text{molCo} \times \frac{1\ \text{mol Co(precursor)} \times 58.93\ \text{Co(precursor)}}{1\ \text{molCo} \times 1\ \text{mol Co(precursor)} \times 0.06}$$

=0.40g.

Calculation for Ti precursor :

$$0.15\ \text{molTi} \times \frac{1\ \text{mol Ti(precursor)} \times 340.32\ \text{Ti(precursor)}}{1\ \text{molTi} \times 1\ \text{mol Ti(precursor)} \times 0.9999}$$

= 52.63 g.

For monometallic catalyst, the 0.5%Pt/TiO_2 catalysts prepared by impregnation method was shown.

Reagents: Platinum(II)acetyl-acetonate 99.99%

Titanium(IV) butoxide reagent grade, 97%

Xylene 99.8%

Based on 2 g of catalysts used, the composition of catalysts will be as follows:

Platinum = (0.5×2)/100 =0.01 g

TiO_2 = 2-0.01 = 1.99 g

Platinum 0.01 g was prepared by using platinum(II)acetyl-acetonate 99.99%

$$= \frac{\text{MW.of platinum(II)acetyl}-\text{acetonate} \times \text{weight of platinum required}}{\text{MW.of platinum}}$$

$$= \frac{323.29\ \text{g/mol} \times 0.01\text{g}}{195.078/\text{mol}}$$

= 0.0201 g.

For monometallic catalyst, the 0.5%Pt-0.04Co/TiO_2 catalysts prepared by Co-impregnation method was shown.

Reagents: Platinum(II)acetyl-acetonate 99.99%

Titanium(IV) butoxide reagent grade, 97%

Cobalt naphthenate, 6 wt% in mineral spirits

Xylene 99.8%

Based on 2 g of catalysts used, the composition of catalysts will be as follows :

Platinum = (0.5×2)/100 =0.01 g

Cobalt = (0.04×2)/100 =8 × 10^{-4}g

TiO_2 or modified TiO2 = 2-0.01- 8 × 10^{-4}= 1.9892 g

Platinum 0.01 g was prepared by using platinum(II)acetyl-acetonate 99.99%

$$= \frac{\text{MW.of platinum(II)acetyl}-\text{acetonate} \times \text{weight of platinum required}}{\text{MW.of platinum}}$$

$$= \frac{323.29\ \text{g/mol} \times 0.01\text{g}}{\frac{195.078\ \text{g}}{\text{mol}} \times 0.999}$$

= 0.0201 g.

Cobalt 8 × 10^{-4}g was prepared by using cobalt naphthenate, 6 wt% in mineral spirits

$$= \frac{100 \times \text{weight of cobalt naphthenate required}}{\%\ \text{cobalt in precuror}}$$

$$= \frac{100 \times 8 \times 10^{-4}\text{g}}{6}$$

= 0.1333 g.

APPENDIX B

CALCULATION OF THE CRYSTALLITE SIZE

Calculation of the crystallite size by Debye-Scherrer equation

The crystallite size was calculation from the half-height width of the diffraction peak of XRD pattern using the Debye-Scherrer equation.

From Scherrer equation

$$D = \frac{K\lambda}{\beta \cos\theta}$$

Where D= Crystallite size, Å

K = crystallite-shape factor=0.9

λ = X-ray wavelength, 1.5418 Å for CuK_{α}

θ = Observed peak angle, degree

β = X-ray diffraction broadening, radian

X-ray diffraction broadening (β) is the corrected width of a powder diffraction free from all broadening due to the instrument. The α -alumina was used as a standard sample to observe the instrumental broadening data. The most common correction for the X-ray diffraction broadening (β) can be obtained by using Warren's formula

From Warren's formula:

$$\beta = \sqrt{B_m^2 - B_s^2}$$

Where B_M = The measured peak width in radians at half peak height

B_S = The corresponding width of the standard material

APPENDIX C

CALCULATION OF THE PHASE COMPOSITION

Phase composition of all catalysts was calculated from:

Weight of anatase as function of

$$f = \frac{1}{1+1.26\frac{Ir}{Ia}}$$

Where Ir = Intensity of rutile TiO_2 phase

Ia = Intensity of anatase TiO_2 phase

APPENDIX D

CALCULATION FOR METAL ACTIVE SITES AND DISPERSION

Calculation of Pt active sites and Pt dispersion of the catalyst by CO-chemisorption is as follows:

Volume of CO adsorption on catalyst, Vads = $\frac{V_{inj}}{m} \times \sum_{i-1}^{n}(1 - \frac{A_i}{A_f})$

Where Vinj = volume injected, 0.02 cm3

m = mass of catalyst used, g

Ai = area of peak i

Af = area of last peak

Pt active sites

Pt active sites = $S_f \times \frac{V_{ads}}{V_g} \times N_A$

Where S_f = stoichiometer factor, CO adsorbed on Pt, CO:Pt=1

V_{ads} = volume adsorbed

V_g = molar volume of gas at STP, 22414 cm^3/mol

N_A = Avogadro's number, 6.023×10^{23} molecules/mol

Metal dispersion

$$\text{Metal dispersion (\%)} = 100 \times \frac{\textbf{molecule of Pt loaded}}{\textbf{molecule of Pt from CO adsorption}}$$

$$\%D = S_f \times \frac{\mathbf{V_{ads}}}{\mathbf{V_g}} \times \frac{\mathbf{MW}}{\mathbf{\%M}} \times 100\% \times 100\%$$

Where S_f = stoichiometer factor, CO adsorbed on Pt, CO:Pt=1

V_{ads} = volume adsorbed

V_g = molar volume of gas at STP, 22414 cm^3/mol

MW = molecular weight of the metal

%M = weight percent of the active metal

APPENDIX E

CALCULATION FOR CATALYTIC PERFORMANCE

Calculation of conversion and selectivity of the catalysts are shown in this below. The calibration curve of furfural and furfuryl alcohol are shown in Fig. E1-E2.

$$\%\text{Conversion} = \frac{\text{Mole (in)} - \text{Mole (out)}}{\text{Mole (in)}} \times 100$$

$$\%\ \text{Furfural conversion} = \frac{\text{Mole of fufural (in)} - \text{Mole of fufural(out)}}{\text{Mole of fufural (in)}} \times 100$$

$$\%\text{Selectivity} = \frac{\text{Mole of product}}{\text{Mole of converted reactant}} \times 100$$

$$\%\text{Furfuryl alcohol selectivity} = \frac{\text{Mole of furfuryl alcohol}}{\text{Mole of converted furfural}} \times 100$$

Reaction result from GC-FID, found that two peaks product consisted of furfuryl alcohol peak and solvent product peak. So solvent product selectivity calculation below equation

$$\%\text{Solvent product selectivity} = 100 - \%\text{Furfuryl alcohol selectivity}$$

$$\%\text{Yield} = \text{conversion} \times \text{selectivity}$$

$$\%\ \text{Furfuryl alcohol Yield} = \text{Furfural conversion} \times \text{Furfuryl alcohol selectivity}$$

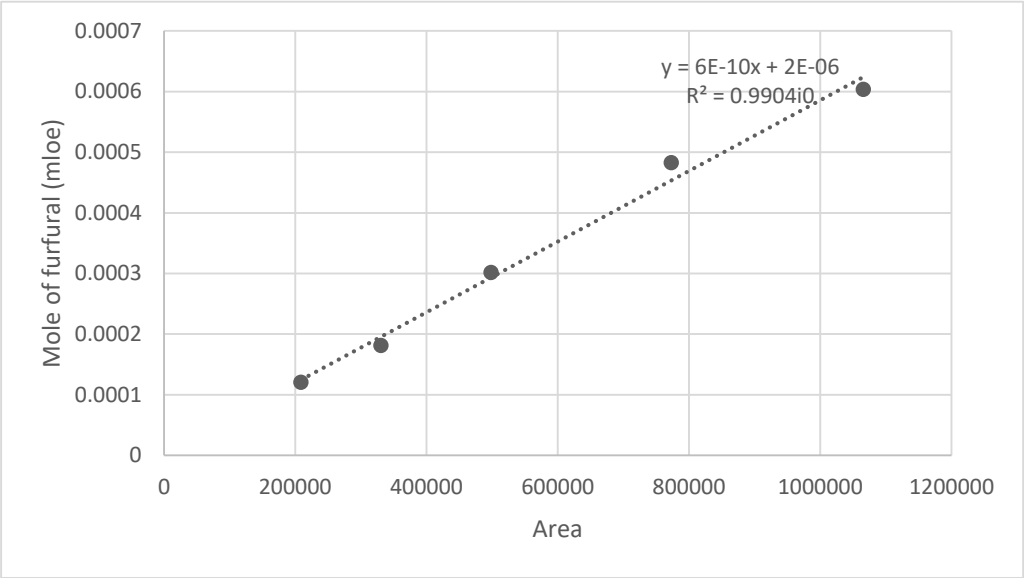

Figure E.1 The calibration curve of furfural

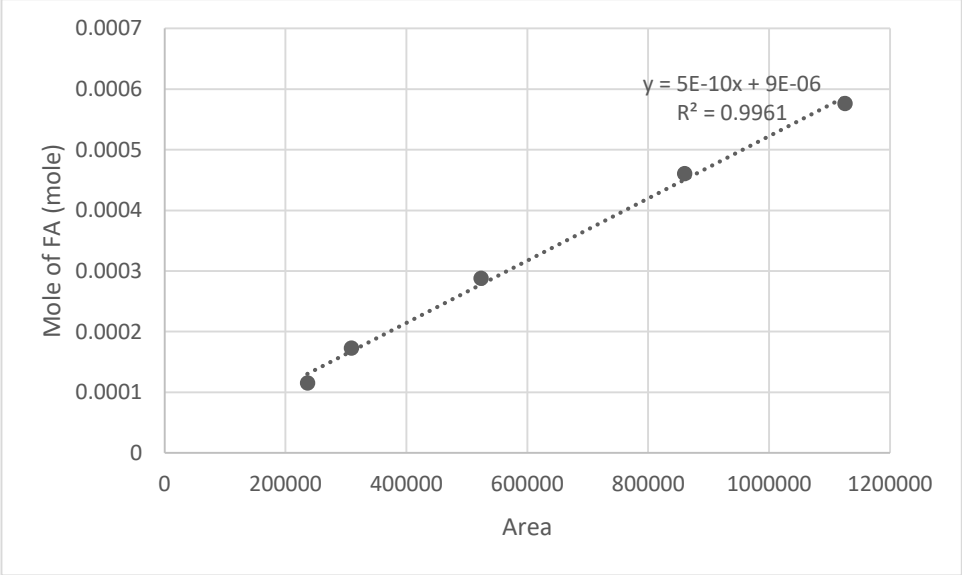

Figure E.2 The calibration curve of furfuryl alcohol

VITA

Miss Kitima Kruachao was born on April 10th, 1994 in Ratchaburi, Thailand. She received the Bachelor's Degree in Chemical Engineering from Department of Chemical Engineering, Faculty of Engineering and Industrial Technology, Silpakorn University, Nakhonpathom, Thailand in March 2016. Thereafter, she entered to study in Master's Degree of Chemical Engineering at Department of Chemical Engineering, Chulalongkorn University, Bangkok Thailand since 2016 and joined center of excellence on catalysis and catalytic reaction engineering research group.